2021

Applying Inverse Dynamics To A Biomechanical Model To Determine The Safety Of The Motogaitor

Ezzuddin Abuhussein
University of Alabama at Birmingham

APPLYING INVERSE DYNAMICS TO A BIOMECHANICAL MODEL TO DETERMINE THE SAFETY OF THE MOTOGAITOR

by

EZZUDDIN ABUHUSSEIN

ALAN EBERHARDT, COMMITTEE CHAIR
JOEL BERRY
CHRISTOPHER HURT

A THESIS

Submitted to the graduate faculty of The University of Alabama at Birmingham,
in partial fulfillment of the requirements for the degree of
Master of Science

BIRMINGHAM, ALABAMA

2021

ABSTRACT

People with mobility impairments caused by conditions such as cerebral palsy (CP), stroke, and spina bifida have difficulty achieving high levels of exercise. The lack of exercise can lead to secondary conditions such as diabetes, obesity, and cardiovascular diseases. Gait-training devices are already commercially available; however, they are not fit for home use and are expensive. Therefore, there exists a need for an affordable gait-training device that is compact and promotes exercise and rehabilitation in a home-setting. A motorized gait-training elliptical dubbed the "Motogaitor," was designed by students to address the needs of people with mobility impairments.

In this present study, we aimed to test methodologies to obtain reaction forces from load cells and marker trajectories from a motion capture system to apply an inverse dynamics routine to quantify net joint moments during walking and while using the Motogaitor. We tested the device on one healthy user and collected ground reaction forces and marker trajectories, which were later used in OpenSim in applying the inverse dynamics routine to obtain frontal and sagittal plane joint moments. We further tested the effects of differential stride lengths during Motogaitor exercise by changing the length of the crank arm on either side of the elliptical. We also created a model that simulates the effects of CP on children while performing the kinematic motion of the Motogaitor.

Our results indicate that Motogaitor exercise generates sagittal plane moments similar to what has been reported in literature. Peak frontal plane moments did not exceed the peaks seen in over-ground walking although they had similar patterns. Lastly, increasing the length of the crank arm causes a descriptive reduction in the internal moments generated and decreasing its length reverses the effects.

TABLE OF CONTENTS

Page

LIST OF TABLES

LIST OF FIGURES

CHAPTER 1

INTRODUCTION

Conditions such as cerebral palsy (CP), stroke, and many neurodevelopmental diseases can cause mobility impairments in people, thus hindering their ability to exercise. Their conditions pose a challenge to them and their caregivers because of their inability to walk independently. Moreover, the lack of exercise and physical activity could lead to cardiovascular conditions, obesity, diabetes, and osteoporosis. Research has shown that increased motor activity leads to improved cardiovascular and mental health, increases cognitive performance, and reduces mortality rate among people. Physical therapy and exercise improve the ability of people to walk and exercise, however, due to financial, physiological, and physical barriers, traditional physical therapy is not efficient for people with severe conditions. Robotic exercise devices are available on the market and studies suggest that elliptical training is the most similar to over-ground walking compared to other types of robotic devices [1]. However, of the available devices on the market, very few are made for a home setting; they lack aerobic and resistance training options in safe environments, which are essential for the rehabilitation process. Also, they do not provide differential resistance (each leg has a different resistance level), which has been proven to correct asymmetry and improve balance in post-stroke patients [2]. Therefore, there is a need for a home-based rehabilitation device that promotes gait-training and physical activity through resistance and aerobic exercise in users

independently and in a safe environment. Using published literature and information from clinicians, a motorized elliptical machine dubbed the “Motogaitor” was developed for a specific child with CP. After conducting user-testing and feedback from physical therapists/caregivers, it was evident that the device should allow the user to ambulate without assistance from the motor if needed, allow for inducing resistance, and contain special foot-plates to ensure that the feet remain attached to the pedals during the exercise without forcing them into unusual positions. Furthermore, to assess post-stroke patients’ needs in adults, we will develop a differential resistance mechanism and implement in in the device in order to correct gait asymmetry in hemiparetic patients. In this study, we discuss some of these design specifications and how they were addressed. Furthermore, we apply inverse dynamics to a biomechanical model using the Motogaitor to estimate joint moments and powers.

CHAPTER 2

LITERATURE REVIEW

People with mobility impairments and neurological muscle coordination issues caused by conditions such as multiple sclerosis (MS), spina bifida, arthritis, and cerebral palsy, are often unable to exercise due to the pain, loss of motor control, reduced selective motor control, and exaggerated reflexes. Their physical disabilities make them less likely to exercise than people without disabilities. In fact, 56% of people with disabilities do not exercise whereas 36% of healthy people exercise. Therefore, it is evident that disabilities lead to physical inactivity which leads to a lack of independence and affects their physical and emotional well-being [4, 5]. Physical inactivity also increases the risk of chronic diseases and causes deficits in health-related physical attributes [6]. The negative effects could range from reduced musculoskeletal flexibility and cardiovascular function to changes in body composition. Other complications include obesity, diabetes, fatigue, and even higher mortality rates [7]. There is a direct relationship between the amount of time spent sitting down with high body mass index (BMI), and there is also a direct relationship between sedentary lifestyles and the risk of acquiring type 2 diabetes. In a study involving 577 people with impaired glucose tolerance (IGT), who more prone to acquiring type 2 diabetes, it has been shown that exercise and healthy diets decrease their progression from IGT to type 2 diabetes by

almost 44%. People with mobility impairments caused by neuromuscular diseases are especially prone to coronary artery disease and osteoporosis [8, 9]. Physical inactivity has also been associated with depression. In a study among adults with MS, spinal cord injuries (SCI), muscular dystrophy (MD), and postpolio syndrome (PPS), there was a statistically significant association between physical activity and lower self-reported depressive symptoms [10]. Contrarily, increased physical activity and daily, low-intensity exercises reduce the risk of falling, and improve physical fitness and aerobic capacity [11]. It also leads to lower mortality rates caused by chronic diseases such as diabetes, lowers the risk for morbidity, improves cardiovascular health, and increases muscle strength and endurance [12]. However, many of these people are unable to exercise due to their impairments, therefore, physical therapy helps them exercise and improves their gait.

For example, there are 10,400 cases of Multiple Sclerosis cases per year who begin experiencing difficulty walking, on average, after 8 years of the diagnosis. Thirty years after the diagnosis the patient will have to use a wheelchair. Overall, more than 50% of people with MS are unable to work and collectively require $16 billion annually for treatments [13, 14]. Similarly, 12,000 to 20,000 incidents of spinal injuries happen each year. The limitations caused by the injury depend on the severity of it, but high cervical injury (C1 – C4) will need to operate a powered wheelchair [15, 16]. The higher the level of spinal cord injury, the more limitations in living and locomotion they will experience. Cerebral palsy (CP) is the most common etiology of movement disorders in the United States, which often causes muscle rigidity and involuntary movements. Every year, approximately 10,000 people are born with CP and 2.5 out of 1000 births are

diagnosed with the condition in the United States alone. Almost 73% of those children are spastic and 41% of them use some sort of a mobility device [17, 18].

The term CP covers a heterogeneous group of disorders and the symptoms overlap with symptoms from other conditions, therefore, this document will focus on CP in children/adolescents and hemiparesis in post-stroke adults.

Cerebral Palsy

The Gross Motor Functional Classification System (GMFCS) classifies CP in children into five levels, ranging from level I to level V, based on their functional mobility (Fig. 1). The classification criteria are the children's functional limitations, use of mobility devices (i.e.: crutches, walkers, etc.), and the use of wheeled devices (fig. 1). Children with CP levels of I and II are often able to walk with minor difficulties, however, children with higher levels (such as GMFCS levels IV and V) face more functional limitations and are the least active [19]. Other assessment instruments used to quantify the development and the motor skills of patients are the Child Health Questionnaire and the Wong-Baker FACES Pain Rating Scale. In addition to physical problems, seizures, growth problems, and neurological abnormalities (impaired vision, abnormal pain reception, etc.) are also common in children with CP. In fact, almost 65% of all patients with CP experience seizures [20].

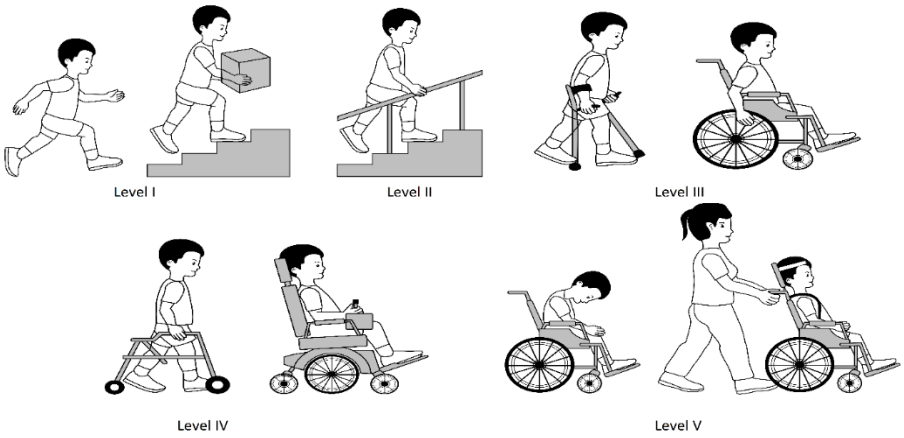

Figure 1. Demonstrates the five levels of CP according to the GMFCS.

CP and mobility impairments, in general, are further classified into one of five groups depending on the affected limbs: Hemiplegia, paraplegia, tetraplegia, diplegia, and monoplegia. Figure 2 shows the affected limbs, highlighted in grey. The patient can lose

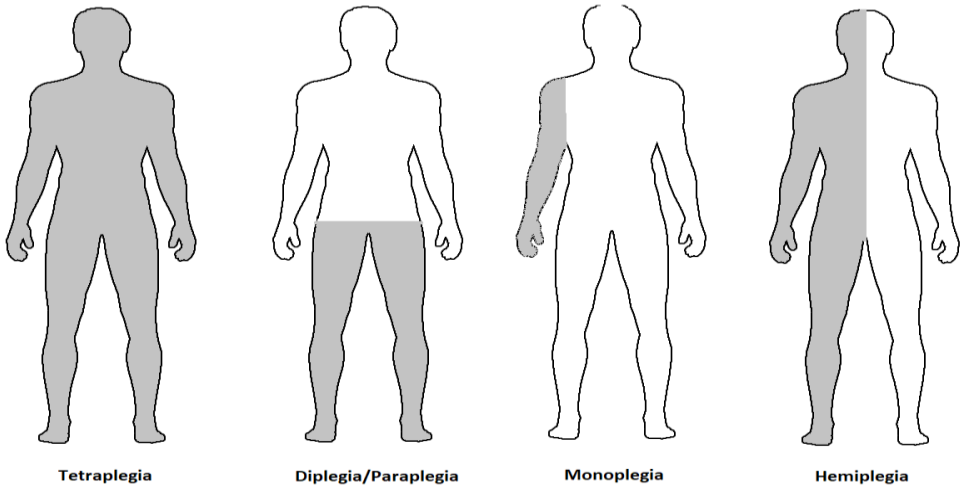

Figure 2. Classification of mobility impairments based on the affected limb(s).

full or partial control in the affected limbs. The focus of this document will be on all groups, but a lower limb must be affected to be considered for the study.

Management and Treatment of Cerebral Palsy

Treatments for people with CP vary with the patient's specific symptoms. They range from medications to physical therapy. The most common type of physical therapy is neurodevelopmental treatments (NDT), which aim at controlling the motor function of muscles, eliminating abnormal patterns, and improving muscle tone and reflexes. This treatment uses guided, repetitive movements to make a particular movement pattern readily accessible for the patient. This type of treatment does improve the gross motor function in children significantly, but the immediate improvements in the dynamic range of motion and the cognitive range of development are not consistent across studies [21, 22]. Physical therapy through muscle strengthening programs is the second type of treatment. Although it was believed that increasing the muscle mass increases the spasticity as well, several recent studies refuted the statements and proved that assistive-resistive exercise is beneficial in muscle strengthening to children with cerebral palsy [23, 24].

Some examples of medications are Botulinum toxin (Botox) and Baclofen. Botulinum toxin type A has been discussed in several research papers, but there is not strong evidence to support or refute its efficiency in the treatment of spasticity [25]. Baclofen has been proven to reduce spasticity in lower extremities, though there is no strong evidence regarding the upper extremities [26].

Increased motor activity through exercise and physical therapy leads to better physical and mental health. They have also shown that motor activity increases cognitive performance and promotes recovery of damaged nervous systems. As such, children with lower limb impairments, and especially those who have CP, should be able to get regular exercise [27]. According to the United States Department of Health and Human Services

(HHS), children and adolescents ages 6 – 17 years should do 60 minutes or more of moderate-to-vigorous physical activity daily. They classify the physical activity as aerobic, muscle-strengthening, and bone-strengthening activities. Each of the mentioned activities should be done at least 3 days of the week [28]. However, children with disabilities are not able to exercise as much. On average, children with physical and other disabilities exercise for 17 ± 4.2 minutes daily. The mean duration of physical activity as reported by the patients and their parents was 3.4 ± 1.9 hours/week, which is significantly less than the recommended time suggested by the HHS [29].

Post-stroke and Hemiparesis

Stoke is the leading cause of disability in adults in industrialized societies. The lifetime risk of stroke in adults 55 years or older; 1 in 5 women and 1 in 6 men are at risk of strokes with a higher risk as they get older [30]. Obesity, diabetes, and elevated blood cholesterol are risk factors associated with strokes, so sedentary lifestyles and bad dietary habits lead strokes. These habits worsen as stroke survivors have a number of functional limitations including muscle weakness, poor balance, and pain. Of the serious motor impairments, hemiparesis affects 65% of stroke patients causing weakness in one side of the body. In comparison with healthy subjects, they show reduced walking speed, reduced strength in flexor muscles and the knee extensor muscles, and asymmetry in walking [31]. One year after a stroke, 30% of patients die and 40% will be dependent on others for their daily activities, which is why physical therapy and treatment are essential [32]. The recovery of walking function varies with patients, but on average, it occurs within the first 6 months after the stroke. It has been reported that through physical

therapy and medication, an independent walking function could be restored in 65% of the survivors [32].

Management and Treatment of Hemiparesis

Clafin et al. describe the techniques/treatments used for the management and restoration of motor function. Some of the treatments include selective serotonin receptor inhibitor (SSRI) antidepressants, constraint-induced movement therapy (CIMT), mirror therapy, and technology-supported training. Though SSRI is prescribed for patients to treat post-stroke depression, its effects on neuronal plasticity promote motor recovery after stroke [33]. The main concept behind CIMT is that restricting the unaffected limb in a hemiparetic patient will force the individual to use the affected limb to complete their daily tasks. Although it has been demonstrated CIMT could lead to improvement in motor and functional abilities, in many studies, it has led to unclear outcomes and it mainly focuses on upper extremities [34]. In mirror therapy, the patient's paretic limb is placed behind a mirror allowing the patient to perceive the reflection of the nonparetic limb as if it were the affected one. Studies involving mirror therapy have demonstrated statistically significant improvements in motor function in post-stroke patients [34]. Technology-supported training mainly focuses on robot-assisted therapy and virtual-reality/immersion. Combined, robot-assisted therapy and virtual reality are used for rehabilitation therapy by providing three components: Enabling assistive/resistive training via motorized mechanical components, providing visual feedback to motivate the user, and immersing/distracting the user while performing their therapeutic exercises.

For people with hemiparesis/hemiplegia who have unsymmetrical gait patterns, a resistive force needs to be applied to their affected limb. This is because they rely on their

healthy leg to compensate for the lack of propulsive force from their affected leg. Studies have shown that assisting the affected limb, though helpful during the exercise, worsens the asymmetry in their gait pattern as they facilitate use-dependent motor learning [35]. However, if a resistive force is applied to their leg during exercise, their stride length increases and their gait becomes more symmetrical. Yen et al. explained that only seven minutes post-exercise, patients were taking longer strides with their affected limb as they are anticipating a resistive force to be applied to that leg. Split-belt treadmill therapy was designed for this purpose. Such treadmills consist of two separate belts, which can move at different speeds and have different resistance settings. The uneven pattern signals the center nervous system to adapt for the walking pattern thus making the gait more symmetrical [35].

Biomechanics of Walking

Gait analysis is essential to the diagnosis and treatment of cerebral palsy and numerous other mobility impairments. It is used to diagnose walking abnormalities and compare them to healthy gait cycles, but also to analyze and quantify improvements in gait cycles pre and post-operations. The normal (healthy) gait cycle consists of two main phases that begin and end with a heel strike. The ground reaction force vector (GRFV) is used as the reference line for all angle measurements in a gait cycle [36]. The stance phase begins with the heel striking the ground and ends with the toes leaving the ground. It lasts approximately 60% of the entire gait cycle. The faster the person is walking, the less time this phase lasts. The swing phase begins when the foot leaves the ground until the next stance phase. It begins with the toes leaving the ground and ends with the heel strike. This phase comprises 40% of the gait cycle. Figure 3 displays the muscles

activated in both phases and the position of the leg during the gait cycle. The gait cycles in the figures are used as the baseline to compare abnormalities in walking [36].

In gait analysis, clinicians typically use motion markers that are placed on the body part(s) of interest and then recorded using an infrared camera. The location of the markers creates a trajectory of each one in 3D [37]. Other techniques/devices used include electromyography (EMG), Electrogoniometers (EGMs), and force platforms. EMG is used to determine muscle activation in experimental studies in gait cycles. It works by stimulating muscles and generating a voltage over time signal which is used to determine the response time and strength of the activated muscle. EGMs are used to quantify joint movements and angles in static and dynamic settings. Its function is similar to strain gauges; the output is typically electrical resistance with respect to time [38, 39]. Force platforms are used to measure the ground reaction forces and their magnitude in gait analysis.

According to Cage et al., the five parameters of normal gait are stance phase stability, swing phase clearance, foot preposition after terminal swing, length of stride, and energy conservation [40]. The next paragraph will explore how some of the symptoms of CP can affect these parameters. If these symptoms remain untreated, especially people with bilateral CP at GMFCS level III or higher, their ability to walk will deteriorate significantly, in addition to experiencing an increase in pain and fatigue and a reduction in balance.

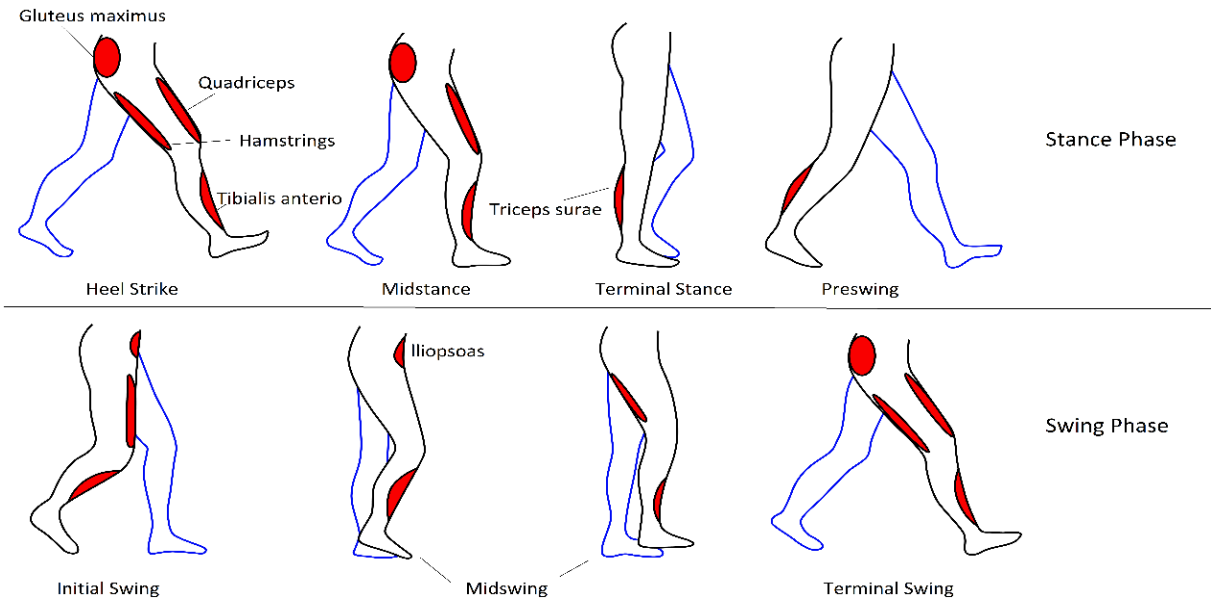

Figure 3. Demonstrates the stages of the gait cycle and the main muscles activated in each stage.

The most common gait problems in children with CP when walking are stiff knee in swing, excessive hip flexion, in-toeing, and equinus, which is the inability to bring the ankle upward at heel strike [41]. The stiffness in knees increases pain and energy expenditure when walking. Quadriceps are activated during the initial contact and loading periods of the stance phase because they stabilize the knee during that phase. Afterward, the quadriceps are relaxed, and the hamstrings muscles are activated to flex the knee at the joint. However, with stiff knees, the quadriceps are forced to be activated during the entire stance phase causing energy expenditure to increase and pressure-caused pain in the knee [41]. From a biomechanical perspective, muscles are classified into three categories: accelerators, shock absorbers, and stabilizers. When walking, a balanced action at the hips, knees, and ankles as well as acceleration from the hips is required to achieve normal gait. The acceleration starts at the hips (quadriceps) when the muscles contract and the hamstrings serve as the decelerators (shock absorbers) by lengthening. Cerebral palsy patients' quadriceps and hamstrings muscles are contracted

simultaneously, which causes their knee stiffness to last throughout the entire walking phase. Thus, they lose the balanced action at their hips, knees, and ankles. This explains their inability to achieve a normal stride length and a normal stance phase stability. Lastly, many CP patients have an equinus foot, which causes poor swing phase clearance; their toes contact the floor first at the end of the swing phase, forcing them to lift their heel and extend their knee. This makes their knee and hips fall behind while their COM advances leading to the twist of the pelvis. CP patients are often prescribed ankle-foot orthosis (AFOs) to correct that. There are several types of orthotics depending on the joints they were designed to contain such as Supramalleoler Orthosis (SMO) and Foot Orthoses (FO). The AFOs are most commonly used by CP patients with spastic diplegia. They control muscle tone and spasticity by providing stability to the joints and maintaining the correct anatomical position [42]. In a gait analysis study involving hemiparetic subjects, AFOs promoted longer, faster strides and better energy conservation when walking [43].

In post-stroke patients, plantarflexion impairment is a major factor in their reduced ability to produce forward propulsion [44]. The weakness/inability to plantarflex leads patients to compensatory strategies such as relying on their nonparetic leg; a nonparetic limb displays significantly higher plantarflexor moment and higher action potential impulse in hemiparetic patients. This causes their COM to advance making their paretic step length longer. Similarly, Hsu et al. found that knee extensors are also stronger in nonparetic limbs as they are used for forward propulsion. Lastly, hemiparetic patients have decreased energy in the pre-swing phase, depicted by reduced action potentials in plantarflexors and hip flexors, resulting in shorter paretic swing time and

stride length [45]. Combined, these limitations affect all five normal gait parameters described to Cage et al.

Manual and Robotic Physical Therapy

Bodyweight supported gait training for people with mobility impairments has increased in recent years. Studies have shown that aerobic exercise training is beneficial in improving aerobic activity and lowers the risk of cardiac complications. Moreover, individualized progressive resistance training increases strength in children and adolescents with spastic diplegic CP [46, 47]. Studies have shown that there is no significant difference between manually assisted bodyweight training and motorized bodyweight training. Furthermore, manual bodyweight training is more labor-intensive and does not provide training-related improvements, which the robotic training provides. Patients who train using automated devices show more improvements in balance, gait symmetry, walking speeds, and fast over-ground walking [47].

Gait-training devices already exist on the market. Weight-supported treadmill training and elliptical machines are especially common. The treadmill is the most similar to over-ground walking; however, elliptical training promotes better cardiovascular fitness in comparison with the treadmill. Elliptical machines, in comparison with cycling and treadmills, have great kinematic similarity to walking, require arm coordination, and are more stable since patients hold onto grips while exercising. Additionally, treadmills require overhead harnesses, which cause some patients to lean forward/backward and rely on the harness system to support their weight rather than using their muscles, which is the goal of physical therapy [48].

The ICARE (Sports Art, Mukilteo, WA) is a motorized elliptical machine and was designed to aid people with conditions that cause mobility impairments such as post-stroke patients, multiple sclerosis, Parkinson's disease, spinal cord injuries, and arthritis. It offers full/partial body weight support through an overhead harness system and provides 40 levels of resistance. It has the option of providing gait training to one or both legs with motor assistance that can be adjusted for each leg. The motor assistance can be in both directions, forward and backward, and it can be turned off, so the user can exercise without any assistance. The ICARE also allows for changing the stride length to accommodate various types of conditions and physical properties (length of legs, muscle strength, etc.) [49]. Studies have shown that the ICARE E872 (Fig. 4) mimics the patterns of walking and improves the patients' cardiovascular health and gait [50]. However, the ICARE was designed for a clinical setting. The device costs more than $30,000 and could be considered large for a home setting.

iCARE Innowalk Lokomat

Figure 4. The E872 ICARE elliptical machine, the Innowalk, and the Lokomat [49, 51, 53].

The Innowalk (Made for Movement, Skien, Norway) shown in fig. 4 is also a motorized elliptical machine, which helps maintain a healthy posture and guide the

movement of the legs and has proven to increase the independent mobility, strength, and balance in patients. There different sizes for various types of patients and encourages passive motion of the lower limbs. The lower back support could be adjusted to be vertical, at an angle, or become a seat and allow the user to perform a cycling motion. It focuses on achieving a biomechanical alignment of the body by providing a variety of supports for the knee, midsection, chest, and head [51]. A study done using the Innowalk suggests that it preserves gait-like movements, improves joint movements, and enhances life quality [52]. It features sensors to detect muscle spasms and disengages when spasms are detected as a safety mechanism. The Innowalk was developed in Norway and costs £12,637 (~ $15,811), which remains expensive.

The Lokomat (Hocoma, Zurich, Switzerland) shown in Fig. 4 is a robotic treadmill that suspends users while their legs are attached to a robotic exoskeleton that mimics walking patterns. It was developed to treat patients with mobility impairments caused by conditions such as neuromuscular disorders, stroke patients, and even cardiac conditions. The overhead harness system that suspends the user allows the physical therapists/caregivers to adjust how much weight is being supported, while the exoskeleton enables them to control patients' walking speed and the amount of assistance provided [53]. Physical therapists can adjust these variables remotely and have a monitor which allows them to track walking patterns and the alignment of the hips and knees. It is different than most gait-training devices in that it eliminates prolonged repetitive movements. Their studies suggest that a modest gait-training intervention with the Lokomat can significantly improve over-ground walking, speed, and gait symmetry [54].

However, like the iCARE, the Lokomat was developed for hospital/clinic setting as it weighs approximately 1000 kg (2204 lb.) and the required space for the LokomatPro is 5 m x 4 m x 2.5 m (196.9 in x 157.5 in x 98.4 in). Furthermore, it costs more than $200,000 to purchase.

The LiteGait (LiteGait, Tempe, AZ) shown in Fig. 5 is a gait training walker designed for children and adults with mobility impairments. It does that by supporting the user's weight and encouraging biomechanically correct posture. It can be used to balance the patients while walking over-ground or a treadmill/elliptical. It also prevents excessive hip rotation while allowing for differential control of the legs. It achieves that by relying on the hip and shoulder harness, which allows for unilateral/bilateral support and enables the clinician to manually assist and guide the patient to achieve the correct gait patterns. The LiteGait was developed with the intention of not only gait training but also enabling the user to walk independently [55].

Figure 5. Displays the pediatric LiteGait and the Rifton Pacer [55, 57].

The most affordable LiteGait device, the LG 75, costs approximately $3000, and it is relatively small, therefore, it is ideal for a home setting, however, a clinician must be present to achieve proper gait training as it is not motorized, unlike the aforementioned

devices. According to Hidler et al., some of its limitations are being heavy, so the patient has to pull it along as they walk, which can be destabilizing. Also, it provides static body weight support rather than dynamic; meaning that the amount of vertical support they experience differs when they are moving because their center of mass (COM) keeps oscillating with the walking motion and the straps holding the harness alternate between being slack and taught. Conversely, dynamic bodyweight support maintains the vertical weight supported constant [56].

The Rifton Pacer (Rifton, NY) shown in Fig. 5 is a walker similar to the LiteGait in that it supports users during over-ground gait training, independent walking, and can be paired with elliptical machine/treadmills and serve as a harness. It has a Multi-Position Saddle (MPS), which helps fine-tune the position of the pelvis to achieve the perfect posture for gait training and encourages forward motion during ambulation. Straps can be installed and tied around the ankles to combat in-toeing, a problem that is common in CP patients.

The Rifton stands out from similar walkers in that it has a dynamic upper frame. Despite still having the issue of being too heavy to pull for some patients, the dynamic upper frame provides dynamic upper weight support, therefore, it accommodates for the shifting of the COM during ambulation, thus achieving more successful gait training. It achieves that by allowing the user's body to slightly move up/down and left/right as seen in walking. Depending on the size of the pacer, the price can start from $745 up to $2,610, making it an affordable option. Still, the device requires the presence of a physical therapist/clinician at all times to achieve proper posture and gait training [57].

Based on the previous examples, it becomes evident that gait rehabilitation systems are limited due to issues in design, cost, and size. Therefore, there is a need for an affordable, ergonomic alternative, which enables users to practice gait and strength training in a home setting safely and with minimum supervision.

CHAPTER 3

PRELIMINARY WORK

The Motogaitor

A motorized pediatric elliptical machine (Fig. 6), the Motogaitor™, was designed and developed by a graduate student for a specific client with level IV CP as defined by the GMFCS. The device was designed with the intention of being used in a home setting, therefore, it is safe, compact, and intuitive. A regular elliptical machine was purchased to serve as the frame and was then modified by adding a NEMA 34 stepper motor (Vevor, China), an Arduino Uno microcontroller, a roller chain, and aluminum footplates with Velcro straps. The motor drives the chain, which drives a crank arm that is connected to the pedals. The microcontroller enables the user to choose between three functions: Forward, backward, and stepping motion. It also provides two-speed settings, starting from 25 RPM to 45 RPM. There is a sliding mechanism in the pedals, which allows the footplates to move forward and backward, making them more accommodating for various physical builds and conditions. Furthermore, the stride length can be adjusted by changing where the pedals connect to the crank arm, thus adjusting the diameter of the ellipse the machine makes and providing differential resistance. Lastly, a smartphone/tablet stand is installed in front of the user to make the experience more engaging or distracting from the workout.

At the time, the Motogaitor allowed the user to exercise by moving their legs for them continuously and for a set amount of time, as chosen by the caregiver. This function was ideal for the level IV CP user as they were unable to walk without a mobility device.

Figure 6. The CAD model of the Motogaitor (left) and the client using the device (right).

User Testing

After getting approval by our Institutional Research Board ((IRB #300003233), user testing of the Motogaitor was done at the Lakeshore Foundation and United Ability, facilities that serve people with disabilities, to assess the device and gain feedback about it from parents/caregivers and physical therapists. Nine users with mobility impairments caused by various conditions tested the device for a minimum of 5 – 10 minutes on the forward function at different speeds as chosen by the therapists/caregivers and the children. They were also encouraged to explore the backward and stepper functions available. Parents/caregivers were given a questionnaire to obtain information about their children such as their physical health (weight, height, exercise habits, etc), their condition and its symptoms, and the type of physical therapy or medication they require. They were additionally asked questions related to the device such as its user-friendliness, safety,

willingness to pay, functionality, and potential improvements. The objective was to make a safe, reasonably priced elliptical machine that meets the users' needs.

Results from the user-testing revealed that there is a need for the device to be commercially available. Users, caregivers, and physical therapists were pleased by the design and its functionality. Their feedback (summarized in Table 1) indicated that children were comfortable with using the machine and parents indicated their willingness to pay between $200 and $5000 for such a device.

Table 1. Feedback from the user-testing that led to the new design constraints.

`	1	2	3	4	5	6
Weight (lbs.)	58	20	23	24	32	36
Height (In.)	48	29	32	N/A	36	38
Age (mo.)	144	16	19	16	24	72
Diagnosis	Level V CP and hydrocephalus	CP - Level unknown	Dandy Walker Syndrome and Developmental Delays	Congenital Hydrocephalus	Left hemiparesis and seizures	Triplegic Spastic CP
Feedback	User Velcro grips similar to Rifton	Better if one person could place child in device	Felt that child was very comfortable in the device	Speed settings are ideal	Could be a little smaller around the waist	Better if it could be interchangeable with variety of walkers and had easier entry
Price	$3,000 to $5,000	N/A	$2000	$2000 - $3000	$200	$1000

Figure 7. The new design concept with the bicycle freewheel sprocket.

The feedback was carefully studied, and a new set of constraints and design specifications were made based on that. The main new need specifications were (1) the ability to “freewheel” without motor assistance, (2) the ability to induce adjustable resistance, (3) having differential resistance so that every pedal has a different level of resistance, (4) the ability to make the grips higher/lower depending on the user’s height/preference, and (5) to cost the buyer less than $3000.

A new design concept (Fig. 7) was made to meet need specifications (1), (2), and (5) was made. The design comprises a motor, a chain, a bicycle freewheel sprocket, and a crank arm. The functionality of the system is the same as the previously mentioned one, however, the addition of the bicycle freewheel sprocket allows the user to exceed the motor speed. The objective is to allow the user to rely on assistance from the motor until they are able to overcome it. This enables the user to exercise for longer periods of time

since they can rest whenever they need to and lets people with different walking capabilities to use the device and still benefit from it.

CHAPTER 4

PROPOSED WORK

The goal is to retrofit the “freewheeling” design to the Motogaitor and ensure its safety and functionality. That includes meeting the general standards for medical electrical equipment in home healthcare environments and in the emergency medical services environments as described by IEC 60601-1 part 1, IEC 60601-1-11, and IEC 60601-1-12. This will ensure that the device meets the general requirements of basic safety and essential performance. Since the electrical components are both protectively earthed and are contained in a box that serves as an additional layer of insulation, its protection is classified as a class II protection. It is further classified as a type B (body) equipment as it operates within the vicinity without touching the patient. Based on these classifications, we have confirmed that it meets the isolation (<1500 Vac), creepage (<2.5 mm), and insulation standards (basic; at least one protective measure), which are the major standards in IEC 60601-1 part 1. As a transportable medical device, IEC 60601-1-12 requires the device to resist Ingress Protection-33 (IP33) without losing function; this means that it should not lose its function if hit by an object of >2.5 mm in diameter or be affected if water drips on it at a vertical angle. Also, the device uses a DC voltage source and since we tested the device during a 30s dip in the voltage from 12V to 10V and the function of the device was not altered, meaning that the device meets the standards described by the document. IEC 60601-1-11 standards for home use, that are not

described by the previously mentioned documents, require the device to have clear instructions, warning signs, an indication of state (i.e.: on/off, operating time, etc.), and the inclusion of a fail-safe mechanism, all of which the device meets.

Using inverse dynamics, the power and moment in the joints will be calculated to ensure the safety and functionality of the device. To apply the method of inverse dynamics, a link-segment model will be created. Certain parameters such as the position of the center of mass (COM) in each segment, radii of gyration, and the relative masses of the segments should be known, but they can be approximated using published literature. The biomechanical model will consist of three rigid segments (thigh, shin/calf, and foot) connected by frictionless pin-joints. Figure 8 displays the forces and moments on a 2-D biomechanical model. The Euler-Newton equations below (1) are used to calculate the forces and moments at the joints in the model:

$$\sum F + mg = ma \qquad (1a)$$

$$\sum M = I\alpha \qquad (1b)$$

where F is the sum of all external forces applied, m is the mass of the rigid body, a is the linear acceleration of the COM, g is the gravitational acceleration, M is the sum of the externally applied moments of force, I is the moment of inertia, and α is the angular acceleration relative to the COM.

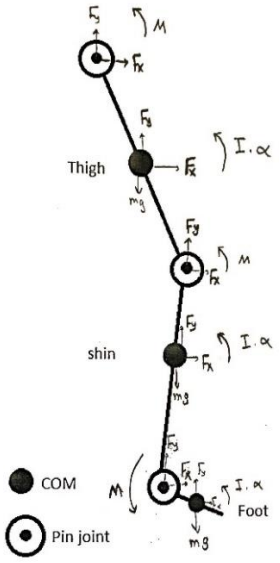

Figure 8. 2-D segmented model of a leg showing the forces and moments at every joint and COM.

In a clinical setting, using (1) and the ground reaction forces from a 6-axis load cell as an input, would enable us to calculate the forces/moments in the joint for each segment. For example, by applying the Euler-Newton equations to the calf segment (figure 9), the following equations (2) will be obtained:

$$F_{joint1} = m(a - g) + F_{joint2} \qquad (2a)$$

$$M_{joint1} = I\alpha - \left(r_{COM} - r_{joint1}\right) \times F_{joint1} + \left(r_{COM} - r_{joint2}\right) \times F_{joint2} + M_{joint2} \qquad (2b)$$

Where r_{COM} is the distance between the COM and the joint.

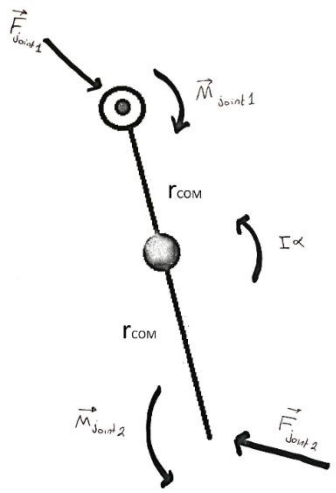

Figure 9. A free-body diagram of the calf segment.

Karatsidis et al. successfully derived general equations (3) to determine the three-dimensional external forces and moments in their 16-segment biomechanical model, which includes the upper leg, lower leg, and the foot. The equations were derived from the Euler-Newton equations described in (1) using only force plates, motion capture systems, and mass ratios and radii of gyration obtained from anthropometric data available in the published literature [58].

$$F_{ext} = \sum_{i=1}^{N} m_i(a_i - g) \qquad (3a)$$

$$M_{ext} = \sum_{i=1}^{N}[j_i\alpha_i + \omega_i \times (J_i\omega_i)] - \sum_{i=1}^{N}\sum_{j=1}^{K_i}(r_{ij} \times F_{ij}) \quad (3b)$$

Where F_{ext} and M_{ext} denote the three-dimensional external forces and moments, respectively, j_i the inertia tensor around the COM of each segment, r_{ij} the position vectors between the COM and the endpoints of each segment, and ω_i is the angular velocity.

The equations in (3) would be applied using custom MATLAB (Mathworks, MA, USA) codes to calculate the forces and moments at the joints. The net joint moment and joint angular velocity will be used to calculate the net joint power as in equation (4a). The calculated power represents the total joint moment to/from all the segments in the model.

However, (4a) is not applicable to biarticular muscles such as the hamstrings because biarticular muscles cross joints and contribute to the net joint power by absorbing/producing power [59]. Equations (4b) and (4c) display how we will calculate the monoarticular and biarticular muscle power.

$$Net\ joint\ power = (M_i \omega_i) \qquad (4a)$$

$$Monoarticular\ joint\ power = M_{muscle} \alpha_{joint} \qquad (4b)$$

$$Biarticular\ joint\ power = M_{muscle,joint\ 1}\ \alpha_{joint,1} + M_{muscle,joint\ 2}\ \alpha_{joint,2} \qquad (4c)$$

Where M_{muscle} denotes the muscle moment at the joint and α_{joint} is the angular acceleration of the joint of interest. The summation of both mono- and biarticular joint powers results in the net joint power.

In our present study, we will implement multi-directional load cells under the footplates to measure ground reaction forces. The user will conduct over-ground walking trials and using the Motogaitor. We will also assess how having differential stride lengths affected the internal joint moments. Joint kinematics and ground reaction forces will be collected to apply the inverse dynamics routine using OpenSim.

Hypotheses

Hypothesis (1) states that the joint kinetics in Motogaitor exercise will resemble elliptical kinetics found in literature. Hypothesis (2) states that changing the length of the crank arm will also change the internal moment at lower extremities. Hypothesis (3) states that the off-axis joint moments will not be descriptively larger in Motogaitor exercise than in walking.

CHAPTER 5

METHODS

Simulated Models

A 4-year-old child, having a height of 40 inches (101.6 cm) and a mass of 35.8 lbs (16.27 kg) was the model for the simulation. Anthropometric data was used to scale the model [61]. As a substitute for marker-based motion data, the CAD rendering was used in Solidworks to perform motion analysis. Markers were placed at the hips, knees, and ankles of the model, and two reference points were placed at the pelvis, which is fixed because of the Rifton Pacer harness system. The simulation was run for one cycle (3 seconds) and the angles were recorded. A video of a child using the Motogaitor was used to approximate the maximum dorsiflexion and plantarflexion angles. Side-view images of the child's feet at the maximum dorsiflexion and plantarflexion were captured from the video and imported into MATLAB. Using the Hough Transform tool in MATLAB, the maximum angles achievable by the ankle joint were approximated. An edge extraction algorithm is applied to the input image, which results in a black/white image. The Hough Transform creates lines along the edges of the white objects and measures the angle of intersection. Figure 10 demonstrates how the image was used to approximate the angles. The joint angles from the motion analysis were then imported into OpenSim using a .mot format, which displays the rate of change of the angles for each joint. Once the model was mobilized, the timeframes of the stance and swing phases were identified in

OpenSim and then in the CAD simulation. The ground reaction forces during Motogaitor exercise were estimated using the finite element method. The contact areas were assumed to be the ball of the foot and the heel based on literature [62].

Figure 10. Hough Transform creating black/white image for edge extraction and angle estimation.

A total of four models were used in OpenSim; one model represented a typically developing (TD) child and the other three each had one of the three most common symptoms present in spastic, diplegic CP level III patients. The three symptoms are knee stiffness in the swing phase, equinus, and in-toeing and exaggerated hip flexion. The models used have 22 segments and 22 joints. Anthropometric data from literature were used to determine the properties of the segments (mass, length, and moment of inertia) and to scale down the model to have the properties of a 4-year-old [63].

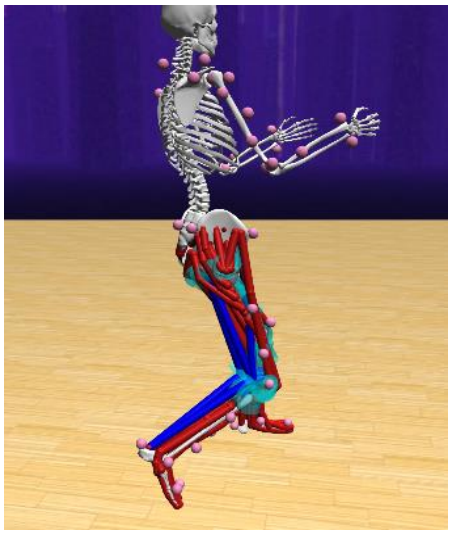

Figure 11. OpenSim model with the spastic muscles associated with the stiff knee (highlighted in blue).

Kainz et al. developed open-source OpenSim models for spastic, diplegic CP patients using experimental data from 12 patients. It uses a MATLAB code that relies on the feedback from the muscle force and its time derivative (force rate) to cause spastic muscle activity. Therefore, muscle force data from the TD model were generated using OpenSim then imported into MATLAB. EMG data were generated using their MATLAB code and were subsequently used in OpenSim for muscle excitations. Through this process, the main knee flexors (mainly the biceps femoris, semitendinosus, and semimembranosus) were excited to achieve the knee stiffness in the swing phase. Figure 11 displays the knee flexors that were affected, highlighted in blue. Using the co-contraction of agonist and antagonist muscles, the stiff knee model was created.

The spasticity of the gluteus maximus and the hamstrings is responsible for the exaggerated hip flexion in the stance phase. It occurs when these muscles are co-activated from initial contact until midstance (0% - 25% of the gait cycle). Similarly, EMG data for

these muscles were used to excite the muscles for 0.75 seconds, which represents 25% of the gait cycle.

Equinus in children with CP could be caused by multiple factors, including contractures of muscles, poor motor control, and ankle joint contracture. Consequently, joint angles from clinical experiments were used to limit the range of motion of the ankle joint and cause excessive plantar flexion. In a long-term study where they examined the effects of tibial neurotomy as a way of treating equinus, it was observed that the average angle of dorsiflexion of the ankle was -0.56 degrees. This value was used to adjust the upper limit of the ankle angle, making it the maximum dorsiflexion possible. Lastly, it has been documented that the most common cause of in-toeing is internal hip rotation. A clinical study with 37 patients with spastic diplegia and quadriplegia showed that the mean value of internal hip rotation is 10.3 °± 8.9°. This value was used to lock the hips at that angle for the model with in-toeing. The goal of the aforementioned steps was to obtain kinematic data (e.g., joint angles with respect to time).

The inverse dynamics (ID) tool in OpenSim was used to determine the torques/moments for the leg joints during the gait cycle. The tool calculates the generalized forces at each joint using the kinematic data, ground reaction forces, and the contact geometry as inputs. The contact geometry was set to be the footplates and the handles, and it determines the magnitude and direction of the ground reaction forces. ID was applied to all four models in addition to over-ground walking models of both CP and TD children. The over-ground walking models are provided by OpenSim. OpenSim displays the gait plots in SI units (N.m, watts, seconds), therefore, Microsoft Excel was

used to convert the outputs to N-m/kg and Watts/kg, and to display the time as a percentage of the gait cycle.

Real Models

Two Axia-80 multi-axis force/torque sensors (ATI Industrial Automation, NC, USA) were installed under the footplates on the Motogaitor to obtain ground reaction forces. Figure 12 displays the sandwiched footplates under the pedals.

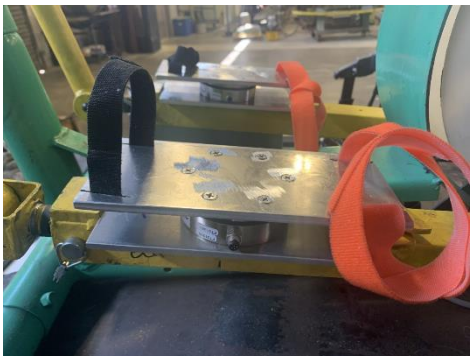

Figure 12. The load cells sandwiched between two plates.

An open-source serial console software called PuTTY (PuTTY, UK) was used to communicate with the sensor. Vicon vantage motion capture cameras (Vicon, Oxford, UK) were used for precision motion tracking to obtain marker trajectories. To sync the data collection, a MOSFET transistor circuit (figure 13) was assembled to send a sufficient signal from the cameras to the load cells.

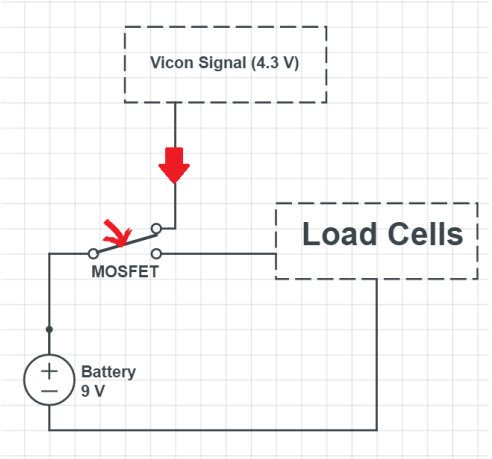

Figure 13. MOSFET circuit where the signal is generated from the Vicon triggering the MOSFET, thus allowing the battery to initiate data collection from the load cells.

To apply inverse dynamics routine and compare the effects of over-ground walking with Motogaitor exercise on joints in lower extremities, thirty-two passive markers were placed on a subject weighing 32.4 kg (71.5 lbs) and 1.4 m (4’7”) in height (figure 14). The motion of the markers was collected by 8 motion capture cameras (Vicon, CO, USA) as the subject walked at a comfortable speed,

in a straight path over two force plates (AMTI, MA, USA) embedded flush with the laboratory floor. The individual performed 5 walking trials resulting in 10 total steps with kinetics and kinematic data collected. Next, we allowed the subject to operate the Motogaitor with their feet strapped in with the motor assistance at the highest setting (35 RPM). We discuss the effects of strapped feet in later sections. The user was instructed to pedal comfortably at a consistent rate with the motor assistance. Five cycles were recorded with both crank arms at level 5 (i.e.: longest crank arm length).

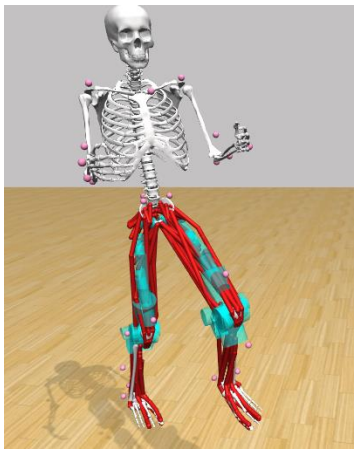

Figure 14. OpenSim model with the markers.

To examine the effects of changing the length of the crank arms of the pedals on joint torques (differential stride lengths), three more trials were recorded. The left leg was set at level 3, which served as a control, while the right leg was set to level 5 in the first trial, then 3 in the second, and 1 in the last trial, as displayed in the diagram in figure 15. Therefore, three trials in total were recorded. The five levels are one inch away from each other each. The collected data from the over-ground walking trial were exported from Vicon's Nexus

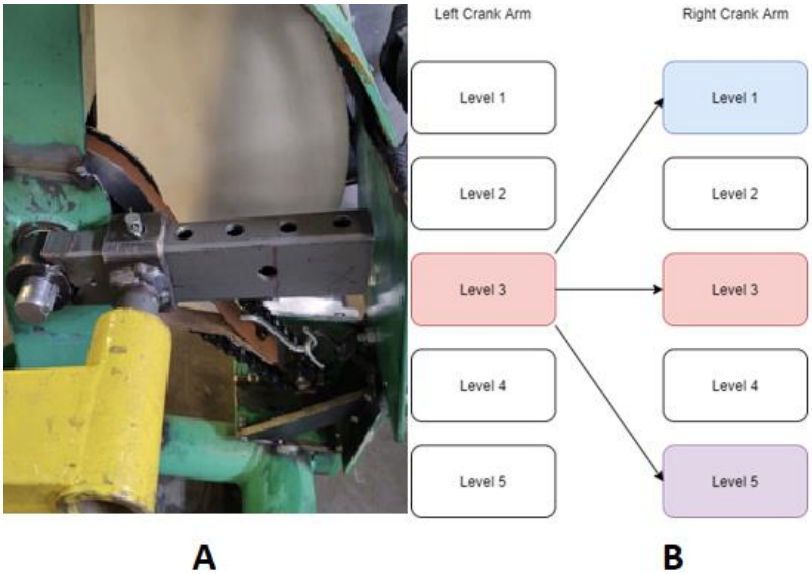

Figure 15. (A) Shows the crank arm. (B) How the trials for the differential stride lengths were performed.3

software in .mot and .trc formats which correspond to the ground reaction forces and marker trajectories, respectively. Similarly, the data from the Motogaitor trials were exported in .trc format from the Nexus software, but the ground reaction forces were obtained from the PuTTY software.

Lee-Son's Toolbox was used to convert Vicon's motion capture data into OpenSim inputs. This toolbox allows the user to adapt the number of makers and their names as well as choosing your global coordinates in the collection volume. An OpenSim model of the subject was created and markers were placed on the model in the exact same locations as the subject in the trials; this step allows for the proper scaling of the model and replication of the subject's movements. Scaling is done by choosing two markers that are placed on joints. These markers are used to define the segment. OpenSim uses the locations of these markers in addition to the participant's weight and height to adjust the length of the segment as well as the weight of it. The collected data was then imported into OpenSim and the Inverse Dynamics tool was used to acquire joint kinetics. The beginning of the stride was set to be the point where the footplate is at its highest position.

CHAPTER 6

RESULTS

Simulated Models

Validation

For validation of the models used in this study, we examined the joint kinetics of the overground walking and Motogaitor joint kinematics in the sagittal plane, and Motogaitor joint moments in the frontal plane. We used the TD model for comparison since no constraints were applied to the model. The data were compared to the available literature. Patikas et al. studied the effects of multilevel surgery on CP patients, pre and post-operation. Gait plots for TD and CP show similar patterns to their findings; the resulting plots were more similar to their gait plots for healthy children [69]. Similarly, Motogaitor joint kinematics in figure 16 were compared to the joint kinematics during exercise using the ICARE. The gait plots for the kinematics were also similar to those of the ICARE in terms of the shape of the graph but the Motogaitor had a narrower range of motion. Lastly, we examined the joint moments in the frontal plane and compared them to the typical lower limb frontal plane moments during over-ground walking [71]. The frontal plane moment plots are displayed in figure 17. Overall, the frontal plane plots resemble what is in literature, however, the generated plots in the frontal plane have descriptively lower peaks compared to the peaks in the study used as a reference. Also,

an unexpected hip abduction moment began to increase at 76% of the gait cycle and reached the peak at 90%.

Concerning Motogaitor joint moments in the sagittal plane, Knutzen et al. examined the effects of changing the ramp position on joint kinetics during elliptical trainer exercise [72]. The hip and knee joint moments and powers in the Motogaitor model are also similar to their findings except for the ankle joint, which resembles over-ground walking kinetics; however, there is a shift in our model making the ankle plantarflexion moment peak at 81% of the gait cycle instead of the expected peak, which typically occurs in over-ground walking at approximately 45% of the gait cycle. The same shift occurs in the ankle joint power plot. Quantitative analysis could not be done given the differences in the physical properties between the model and the subjects in their studies.

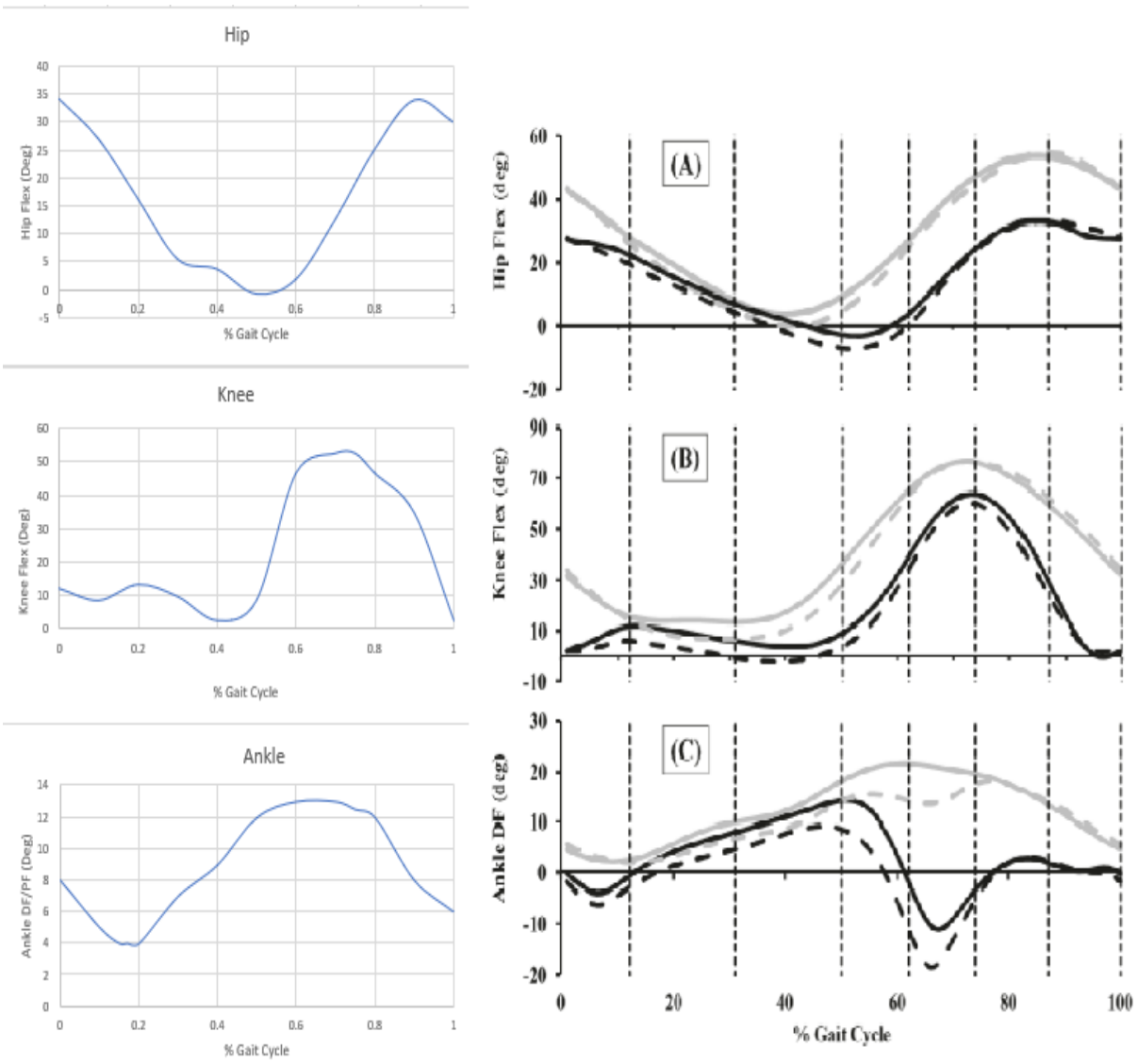

Figure 16. Joint kinematics of the TD model using the Motogaitor in the sagittal plane compared to Buster et al [71].

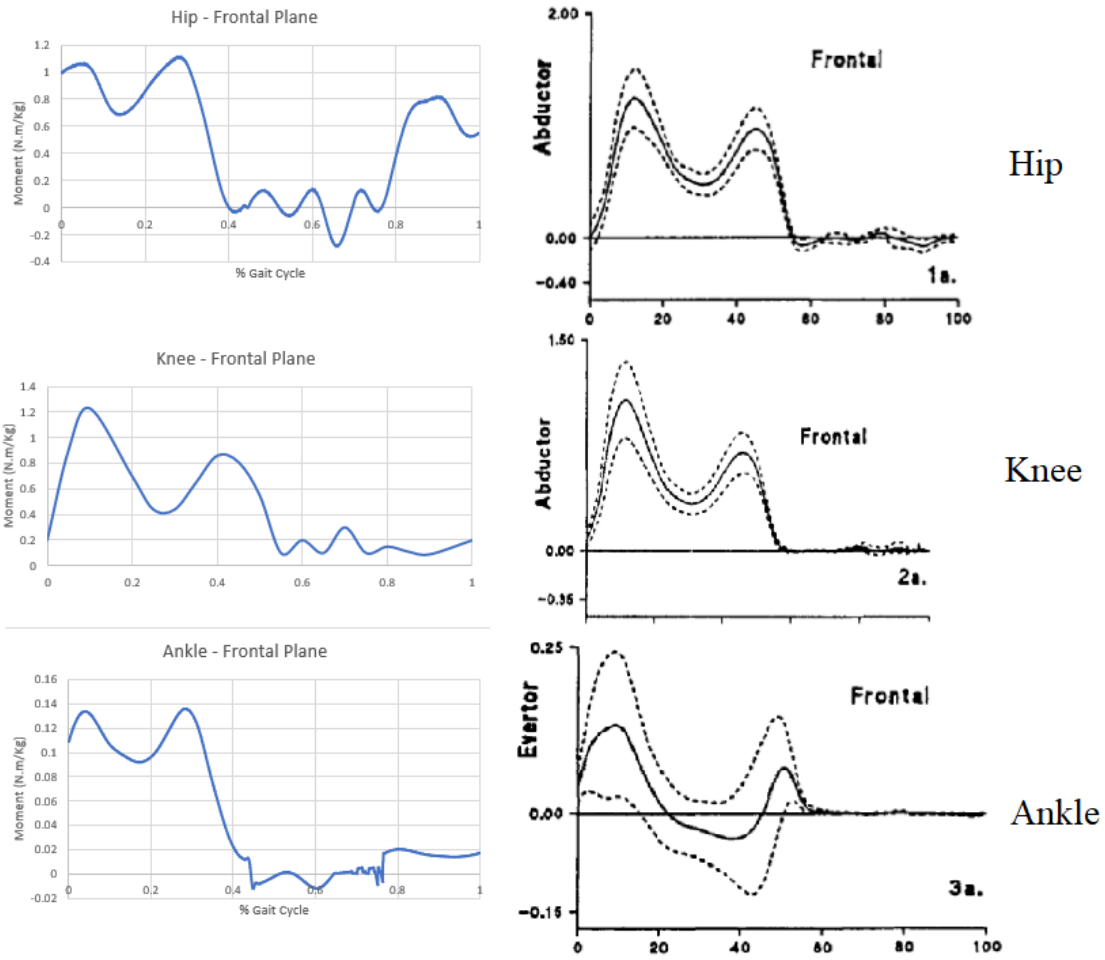

Figure 17. Joint kinetics of the TD model using the Motogaitor in the frontal plane compared to the results of Winter [69].

TD and CP models in Motogaitor exercise

The moments and powers for all three joints during the Motogaitor simulation are displayed in the gait plots in figure 18. Hip moments were descriptively higher in the CP model compared to TD, especially early in the stance phase when the body weight is being fully supported by the stance limb. In the TD model, the peak moment was 0.788 N.m/Kg, compared to 1.35 N.m/Kg in CP. However, it is lower in the swing phase with a peak value of -0.949 N.m/kg for TD and -0.320 Nm/kg for CP. Therefore, there is a higher extensor moment but a lower flexor moment in the hips in the CP model. The

power production at the hip joint in the early stance phase is higher in CP at 1.892 W/kg compared to 1.19 W/Kg) in TD. Knee flexion moment was also descriptively higher in the CP model compared with the TD, reaching 1.45 N.m/Kg in the CP model compared with 1.01 N.m/Kg in the TD. The power generation at the knee joint in the loading response phase is higher in CP (peak value = 1.45 W/Kg) relative to TD (peak value = 1.01 W/kg). In the ankle, there is a larger dorsiflexion moment in TD (peak value = -0.138 N.m/Kg) and more plantarflexion moment in CP (Peak value = 0.119 N.m/Kg) at 74% of the gait cycle. There is also greater power generation in the ankle for TD (peak value = 1.134 W/Kg) during the push-off phase relative to CP (0.84 W/Kg).

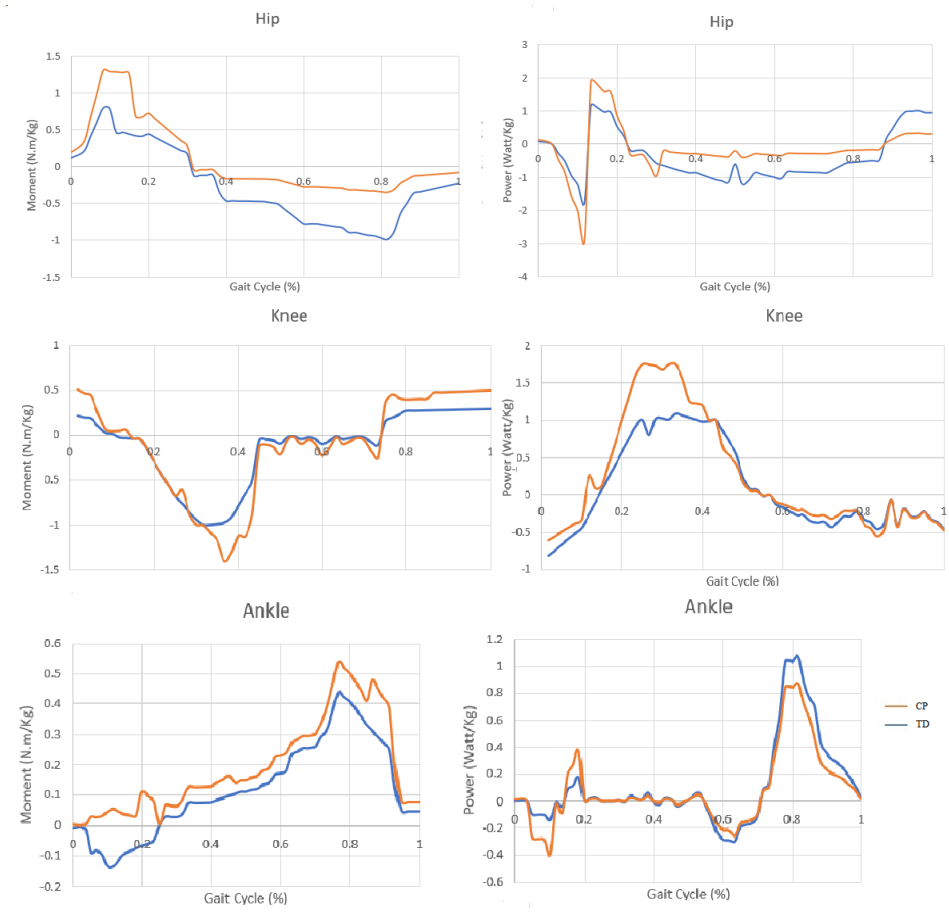

Figure 18. Moment and power gait plots for the CP and TD models in the Motogaitor simulation.

TD and CP Models in Normal Walking

The moments and powers for all three lower-extremity joints during overground walking are displayed in the gait plots in figure 19. In overground walking, the hip joint displayed a flexion moment starting at 19% of the gait cycle. The CP model showed more negative moment (peak value = -1.22 N.m/Kg) relative to the TD model (peak value =-0.549 N.m/Kg).Similarly, CP had a higher extension moment in the swing phase (CP peak value = 1.17 N.m/Kg, TD peak value = 0.539 N.m/Kg). The power in the hip joint during the loading response was descriptively higher in CP (peak value = 2.22 W/Kg) compared to TD (peak value= 1.56 W/Kg). In the knee joint, the moment plot for both models showed similar patterns except towards the end of the stance phase as TD had a much lower peak value relative to CP (TD peak value = -0.779 N.m, CP= -0.261 N.m/Kg). There was an unexpected peak of positive power that replaced the negative power of the K1 region of the gait cycle. For TD, peak value was 0.674 W/Kg compared to CP (Peak value=0.800 W/Kg). The positive power value corresponds to the concentric knee extensor activity during the loading response. There was also a second negative peak in power at 40% of the gait cycle. The values for the TD and CP models were -0.822 W/kg and -0.625, respectively. For the ankle joint, the gait plot for the moments is typical for ankle joints for both models during over-ground walking. The peak value for the TD is 1.20 N.m/Kg and 1.125 N.m/Kg for the CP. In the power plots, there is a negative power corresponding to eccentric plantar flexor activity during the midstance and terminal stance. The peak power values in the propulsive plantarflexion phase during pre-swing are 2.39 W/Kg for the healthy and 1.16 W/Kg for the CP. The value is descriptively lower in the CP and the peak lasted longer than the healthy model.

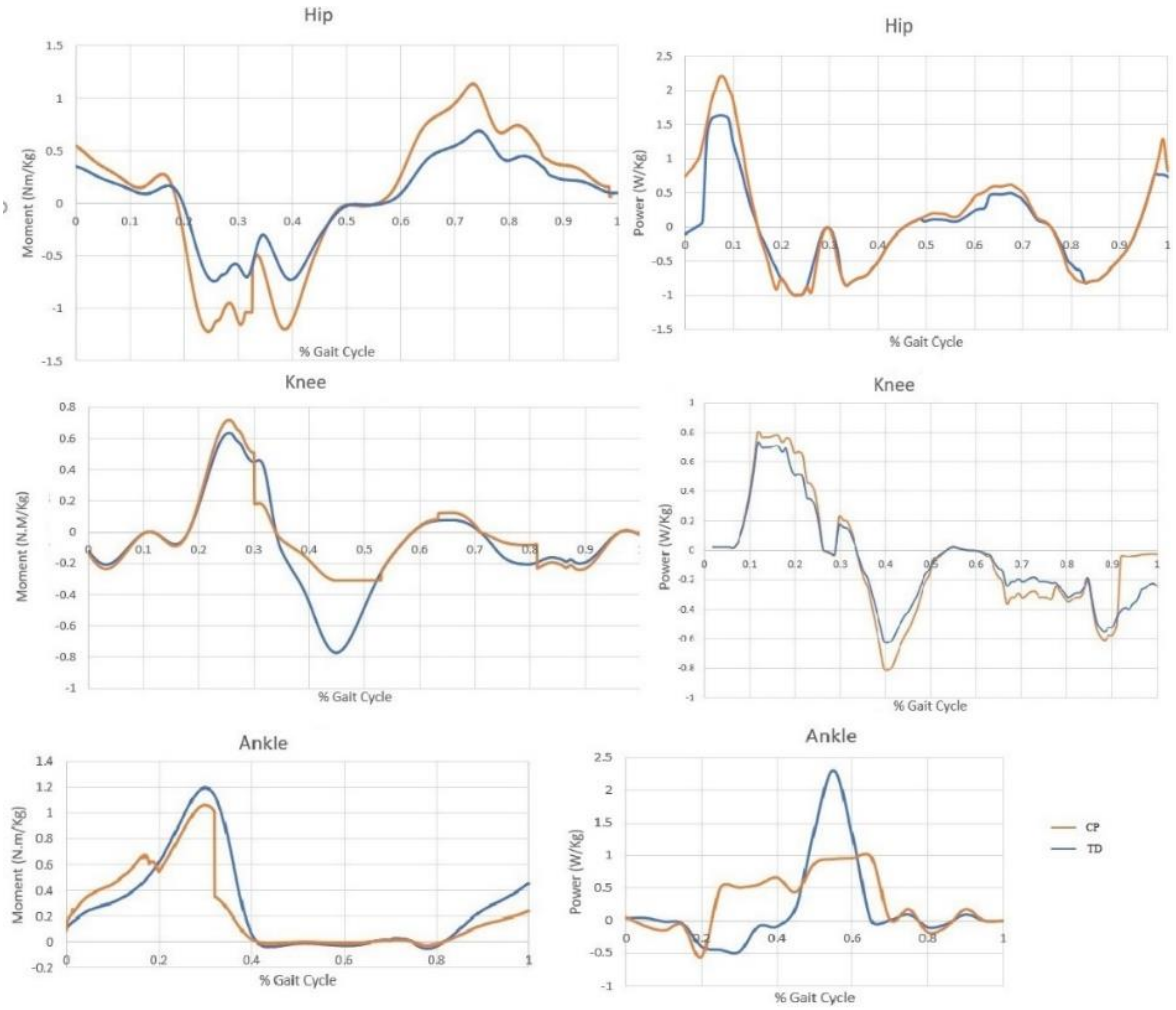

Figure 19. Moment and power gait plots for the CP and TD models during normal walking.

Comparison between the Motogaitor and over-ground walking

I. Hip joint

Abbreviations:

TD: Typically Developed	E: Extensor Moments
F: Flexor Moments	CP: Cerebral Palsy
G: Power Generation	M: Motogaitor Exercise
A: Power Absorption	W: Over-ground Walking

E.g.: M-TD-E: Extensor moments in typically developed children during Motogaitor exercise

In Motogaitor exercise, the gait cycle begins with an extensor moment during the loading response followed by a flexor moment during the swing phase. Peak extensor and flexor moments for the hip joint are displayed in Table 2. Conversely, in over-ground walking, the cycle begins with a flexor moment followed by an extensor

moment later in the swing phase. Peak extensor moments were larger in CP than TD for the Motogaitor and overground walking (M-CP-E=1.35 N.m/Kg, W-CP-E=1.37 N.m/Kg). Peak flexor moments were larger in TD than CP during Motogaitor exercise and lower in over-ground walking (TD-M-E=0.949 N.m/Kg, TD-W-E=0.549 N.m/Kg). In the power plots, there is a descriptively higher absorption in TD during Motogaitor exercise for most of the gait cycle and less power generation peak during over-ground walking (M-TD-A =-1.25 W/Kg, W-TD-A=1.56 W/Kg). In both cases, with the exception of the power generation peaks at the beginning of the cycle (M-CP-G= 1.892 W/Kg, M-CP-G = 2.22 W/Kg), the overall power is less in TD in Motogaitor exercise and similar in over-ground walking.

Table 2. Peak moments in the hip joint in over-ground walking and Motogaitor exercise for TD and CP.

	Motogaitor				Over-ground walking			
	TD		CP		TD		CP	
Moment type	Extensor (+)	Flexor (-)	Extensor (+)	Flexor (-)	Extensor (+)	Flexor (-)	Extensor (+)	Flexor (-)
Moments (N.m/Kg)	0.788	-0.949	1.35	-0.32	0.539	-0.549	1.37	-0.549

II. Knee joint

The Motogaitor moment plot begins with a knee flexor moment followed by an extensor moment at 74% of the gait cycle, whereas the over-ground walking begins with a knee extension moment followed immediately by a hip flexion moment. Peak extensor and flexor moments for the knee joint are displayed in Table 3. Extensor moments for both CP and TD in the Motogaitor model were less than the over-ground walking (M-TD-E = 0.383, M-CP-E = 0.488, W-TD-E = 0.67, W-CP-E = 0.722). However, peak flexor moments were larger in Motogaitor exercise than in over-ground walking with CP being larger than TD in the Motogaitor model and descriptively lower in the over-ground walking model. The power plots display a power generation peak in the Motogaitor

model and two peaks for the over-ground walking. The power generated in the Motogaitor model for both TD and CP was 64.5% more than that of over-ground walking in CP and 55.2% more in TD.

Table 3. Peak moments in the knee joint in over-ground walking and Motogaitor exercise for TD and CP.

	Motogaitor				Over-ground walking			
	TD		CP		TD		CP	
Moment type	Extensor (+)	Flexor (-)	Extensor (+)	Flexor (-)	Extensor (+)	Flexor (-)	Extensor (+)	Flexor (-)
Moments (N.m/Kg)	0.383	-1.01	0.488	-1.45	0.67	-0.78	0.722	-0.31

III. Ankle Joint

For the ankle joint, the peak extensor moment was descriptively higher in Motogaitor exercise and over-ground walking, but there was a shift in the peak moment in Motogaitor exercise making it occur at 74% of the gait cycle instead of early in the stance phase. Peak extensor and flexor moments for the ankle joint are displayed in Table 4. Flexor moments were negligible except in the Motogaitor model in TD (M-TD-E = 0.437 N.m/Kg). Peak extensor moments were lower by approximately in the Motogaitor model than the over-ground walking one; there was a 91.2% difference in TD and 74.5% difference in CP. Also, CP had a higher extensor moment compared with TD in Motogaitor exercise yet a lower moment in over-ground walking (M-TD-E=0.437 N.m/Kg, M-CP-E=0.521 N.m/Kg, W-TD-E=1.17 N.m/Kg, W-CP-E=1.14 N.m/Kg). The power plots show that the power generation was higher in over-ground walking than in Motogaitor exercise. TD had higher power generation than CP in both cases, but there was a bigger difference in the over-ground walking (TD = 1.134 W/Kg, CP=0.84 W/Kg) than in Motogaitor exercise (TD=2.39 W/Kg, CP =1.16 W/Kg).

Table 4. Peak moments in the ankle joint in over-ground walking and Motogaitor exercise for TD and CP.

	Motogaitor				Over-ground walking			
	TD		CP		TD		CP	
Moment type	Extensor (+)	Flexor (-)	Extensor (+)	Flexor (-)	Extensor (+)	Flexor (-)	Extensor (+)	Flexor (-)
Moments (N.m/Kg)	0.437	-0.138	0.521	N/A	1.17	0.02	1.14	0.009

Real Models

1) Net Joint Moments in Overground Walking Compared to Motogaitor Exercise

a) Sagittal Plane

Differences in the net joint moments were observed in all three joints, especially in the knee joint. A complete overview of all net joint moments is displayed in Table 1. Figure 20 contains the gait plots. Higher extension and flexion moments were observed in the hip joint during walking compared to Motogaitor. The peak flexor moment was reached at around 55% of the gait cycle in walking and at 25% in Motogaitor exercise.

In Motogaitor exercise, the moment at the knee remained positive throughout the gait cycle (extensor moment) while walking showed the typical gait pattern. The peak extensor moments were 0.250 Nm/kg and 0.299 Nm/kg for walking and Motogaitor, respectively.

The peak ankle moment was 1.10 Nm/kg in walking and 0.211 Nm/kg in Motogaitor exercise. In walking, there is a gradual increase in plantarflexion moment that reaches its peak at the end of the stance phase. In Motogaitor exercise, the peak occurs at around 25% of the gait cycle, but is significantly lower than the moment in walking.

Table 5. Sagittal plane joint moments during walking and Motogaitor exercise.

Exercise Type	**Hip Moment (Peak)**	**Knee Moment (Peak)**	**Ankle Moment (Peak)**
Walking	-0.520 N.m/kg	0.250 N.m/kg	1.10 N.m/kg
Motogaitor	-0.401 N.m/kg	0.299 N.m/kg	0.211 N.m/kg

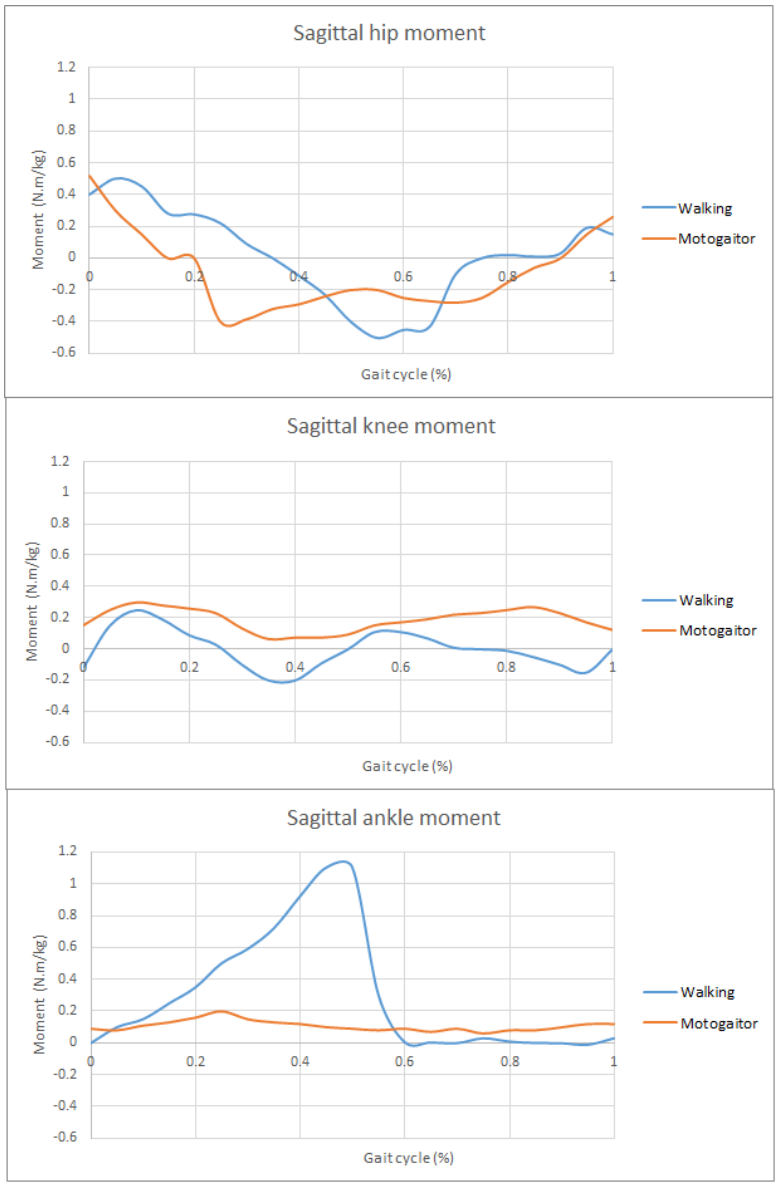

Figure 20. Compares sagittal plane joint moments in walking and Motogaitor exercise.

b) Frontal Plane

Frontal plane moments for all joints are displayed in figure 21. Peak values are shown in table 3. All moments in the frontal plane showed the same pattern with two major peaks in the gait cycle; one higher peak at initial contact to mid-stance and a second peak at terminal stance and early initial swing. At the hip joint, the highest moment peak for walking was 1.16 N.m/kg compared to 1.04 N.m/kg in Motogaitor.

There was a small adduction moment in walking in initial swing, but no adduction moment was observed in Motogaitor. The highest peaks at the knee joint were 1.08 N.m/kg in walking and 0.926 N.m/kg in Motogaitor. Frontal plane ankle moments were drastically lower than the moments at the hips and knees. Low amplitude inversion moment was observed during the first 20% of stance before becoming eversion at around 40% of the cycle. The maximum peaks recorded for the moment are 0.23 N.m/kg during walking and 0.168 N.m/kg in Motogaitor.

Table 6. Frontal plane joint moments during walking and Motogaitor exercise.

Exercise Type	**Hip Abduction Moment (peak)**	**Knee Abduction Moment (Peak)**	**Ankle Inversion Moment (peak)**
Walking	1.16 N.m/kg	1.08 N.m/kg	0.23 N.m/kg
Motogaitor	1.04 N.m/kg	0.926 N.m/kg	0.168 N.m/kg

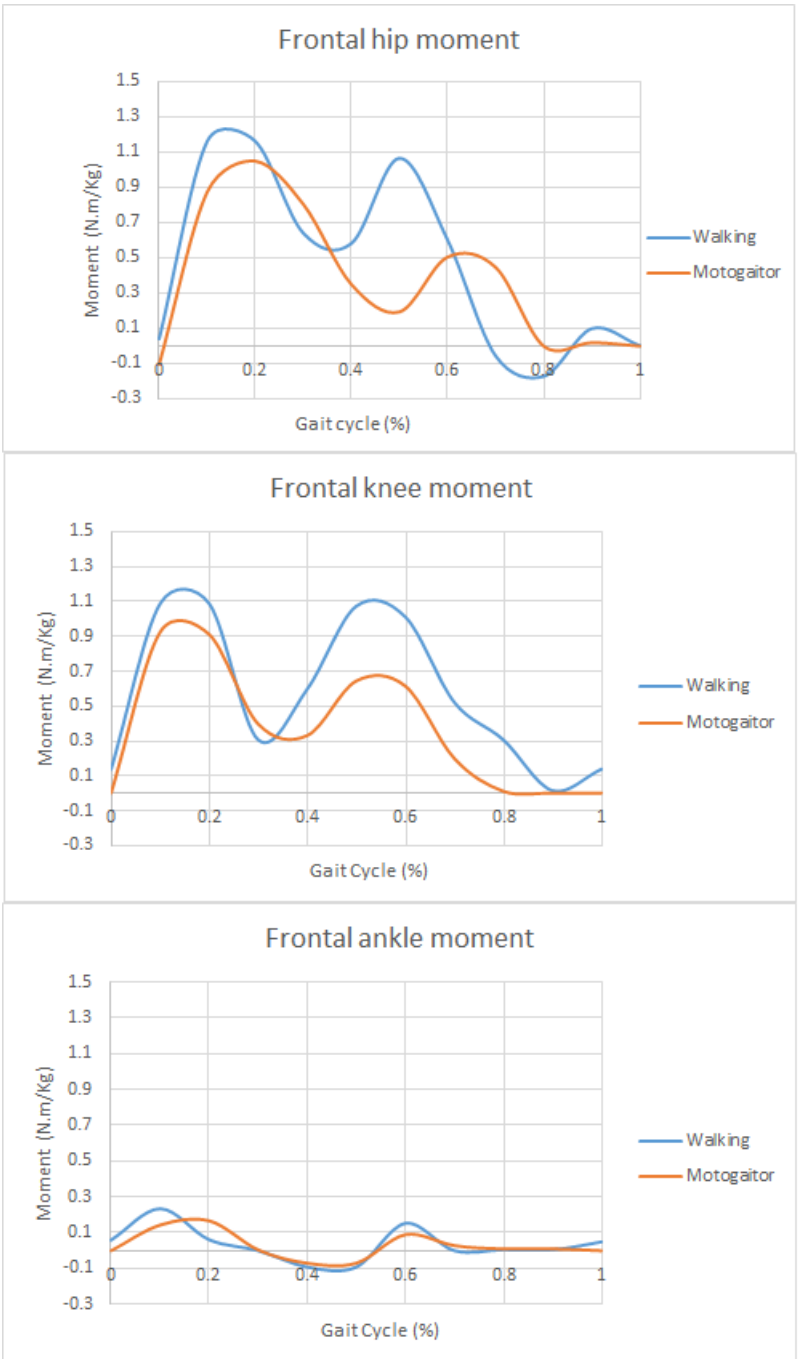

Figure 21. Compares frontal plane joint moments in walking and Motogaitor exercise.

2) The Effects of Differential Stride Lengths on Joint Moments

The joint moments across all three trials will be examined in the next three subsections, where "level" refers to the length of the crank. Level 5 refers to the longest crank arm length whereas level 1 refers to the shortest crank arm length. A complete

overview of all peak joint moments is shown in figure 22. Figure 23 displays the change in joint moments in all joints across the different trials.

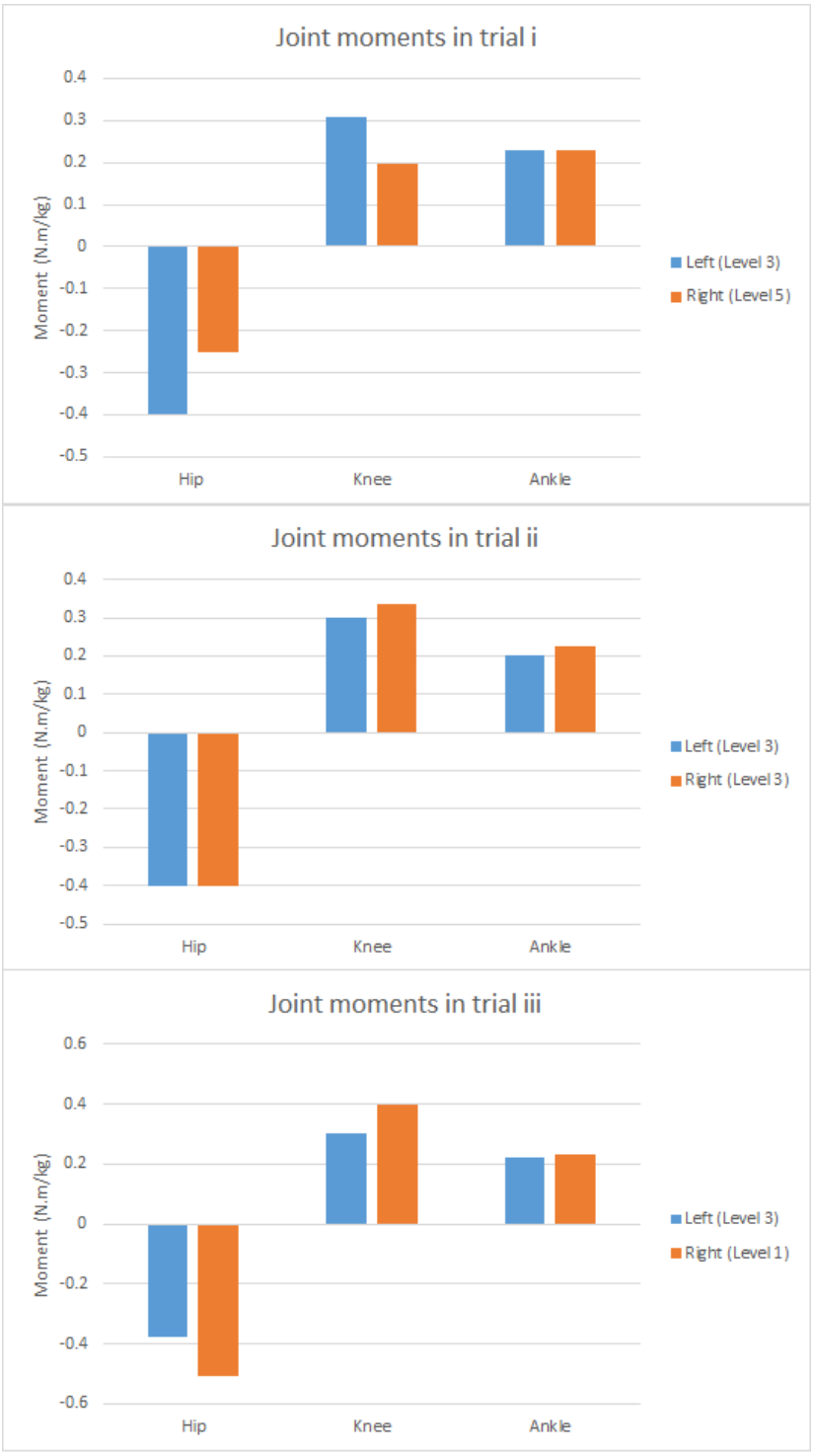

Figure 22. Displays the change in peak joint moments in both legs with the change in crank arm length.

Figure 23. Joint moments due to the change in crank arm length in Motogaitor exercise.

i) Left pedal: Level 3; right pedal: level 5

Similar trends were observed in both legs across all three joints. The flexor moment at the hips reached the peak at around 25% of the gait cycle, but the moment at the left hip was larger by 0.15 N.m/kg.

Two peaks occurred in the knee gait plot. The larger at the knee joints occurred at 15% of the gait cycle and the moment was descriptively higher in the left knee than the right knee. The peaks were 0.31 N.m/kg and 0.198 N.m/kg at the right and the left knee, respectively. Lastly, the peak ankle plantarflexion moments were similar and had the values of 0.23 N.m/kg. No major differences were observed in shape of the gait plot.

ii) Left pedal: Level 3; right pedal: level 3

The hip flexion moments were similar in shape and magnitude in both legs. The flexion moments in the left and right legs reached their peaks in the single-support phase between 20% and 30% of the gait cycle and had the values of -0.39 N.m/kg and -0.4 N.m/kg, respectively.

Similar to walking, knee extension moments had two peaks; one occurring at 10% of the gait cycle and one occurring at 85% of the gait cycle. The maximum value reached was 0.3 N.m/kg in the left knee and 0.336 N.m/kg in the right one.

The peak ankle plantarflexion moment was 0.2 N.m/kg for the left ankle and 0.225 N.m/kg for the right ankle. The net joint moments gradually increased at both ankles from the beginning of the stance phase until the peak at mid-stance where the peak was reached.

iii) Left pedal: Level 3; right pedal: level 1

Descriptive differences between the two legs were recorded in the hip and knee, but not the ankle. The peak hip flexion moment was -0.376 N.m/kg and -0.51 N.m/kg for the left and right hips, respectively. The flexion moment at the right hip remained higher than the moment in the left leg for more than 60% of the gait cycle.

As for the knee joint, both gait plots were similar with the peaks occurring at 10% and 80% of the gait cycle. However, the second peak was descriptively larger in the right leg than the left and had the values 0.398 N.m/kg and 0.28 N.m/kg, respectively.

The peak plantarflexion moment was 0.221 N.m/kg in the left leg and 0.230 N.m/kg in the right leg. There was a delay in the peak dorsiflexion and plantarflexion moments in the left leg compared with the right leg. Both peaks occurred between 30% - 35% of the gait cycle (heel rise).

CHAPTER 7

DISCUSSION

Simulated Models

The angular joint kinematics, frontal plane kinetics, and sagittal plane kinetics of the Motogaitor were in range of the findings presented by Buster, Eng, and Knutzen [69, 70, 71]. Walking kinetics also closely matched the study done by Patikas et al. in terms of pattern and were within range of kinetics for other exercises [69]. The sagittal plane joint moments in the Motogaitor simulation more closely resembled ascending stairs than walking, especially for the hip and knee joints.

Compared with the walking model, the hips begin with an extensor moment and end with a flexor moment. CP exceeds TD in extensor moments in both cases, but the flexor moment is descriptively smaller in the Motogaitor model. The range for the moments is very similar in the two exercises yet the difference in extensor moments between TD and CP was 52.6% in the Motogaitor and 87.1% in over-ground walking. This implies that the moments in the hips increase due to crouch gait and more so during Motogaitor exercise. The knee moment plot in the Motogaitor model displayed a high flexor moment towards mid to terminal stance. The magnitude of flexor and extensor moments was higher in CP, but the overall pattern of the cycle was similar to TD. Having a delayed peak in the knee moment with a high magnitude is indicative of a compensatory alteration in its function caused by the changes in functions in the hips and

ankles. The change in moments in the ankle joint was considerably low in comparison with the hips and knees, but CP was higher than TD in the Motogaitor model. The magnitude of the plantarflexion moment was also descriptively lower in the Motogaitor model than normal walking. The low magnitude is not surprising because of the closed kinetic chain that the foot maintains throughout the cycle due to the straps and pedals. The shift in the plantarflexor moment closely resembled the delayed plantarflexor moment observed in patients with prosthetic feet/legs with solid ankle joints. Kodd et al. suggest that the phase shift in the flexor moment could increase the demands of the muscles controlling the knee joint as well as oxygen consumption, which explains the observed high knee flexion moment [75].

Real Models

The aim of this study was to establish the test methodologies to obtain reaction forces from load cells and marker trajectories from a motion capture system to apply an inverse dynamics routine to quantify net joint moments during walking and while using the Motogaitor. These trials will assist us in understanding the long-term effects of Motogaitor exercise. We compared the net joint moments during Motogaitor exercise with over-ground walking and investigated the effects of changing the length of the crank arm on the joint moments (differential stride lengths). This was achieved by applying inverse dynamics using OpenSim and experimental data.

In comparing the Motogaitor with over-ground walking, the peak hip moment was larger by 0.119 Nm/kg in walking. The gait plot for the hip during walking has the typical characteristics of the hip moment curves seen in literature. It begins with an internal hip extensor moment in early stance and turns into a flexor moment in late stance. In

Motogaitor exercise, the hip moment changes from extensor to flexor at around 20% of the gait cycle and reaches the peak before 25%. This is expected since the shape of the hip moment plot is heavily influenced by the position of the hip relative to the foot and at 25%, the hip is behind the foot so the ground reaction forces pass in front of the hip [61]. In walking, the knee moment curve has the typical early stance and late stance peaks with the largest internal moment being 0.250 N.m/kg compared to Motogaitor which generated an extensor moment of 0.299 N.m/kg. Motogaitor exercise had a similar curve, larger extensor moments, but it did not have any flexor moments. The closed kinetic chain motion seem to constrain the swing limb thus limiting the knee flexion that occurs in late swing and early stance. The greater extensor moments in Motogaitor indicate that there was an increased loading for the quadriceps muscles as a result of the downward slope of the pedals as reported by Lay et al [62, 63]. The ankle had a very different moment curve in Motogaitor compared to walking. After the initial contact in walking, the center of pressure moves forward and the ground reaction forces act to dorsiflex the foot. This causes a rise in internal plantarflexion moment, which can observed in the over-ground walking curve [64]. The excessive hip and knee flexion which occur during elliptical exercise cause the ankle joint to continue to dorsiflex instead of plantarflex. It has been previously reported that the lack of mobility of the ankle in elliptical exercise affects resultant ground reaction forces during pedaling [65].

Our results of the frontal plane moments were consistent with existing literature [61, 62]. The same patterns were observed across all plots. Walking generated higher abduction moments at the hips and knees compared to Motogaitor. This is especially true for the second peak which occurred at initial to mid swig in Motogaitor and in later

stance in walking. Although the peak moments at the ankles were somewhat similar values in walking and Motogaitor, we did not observe a large second peak at pre-swing in Motogaitor. The observed patterns in frontal plane moments between walking and Motogaitor indicate that overall, Motogaitor exercise generated lower off-axis joint moments than walking. Since our main concern is to avoid excessive joint moments relative to walking that could reduce the quality of exercise in the motogaitor and increase risk of soft tissue injury over time [63, 64], our results provide preliminary insight indicating that joint moments during Motogaitor exercise fall within range of over-ground walking.

The effects of differential stride lengths were evident across the three trials. The curve patterns remained the same but there were major differences in magnitude in trial I and III. In trial I, the right leg which had the longer crank arm length had on average lower extension and flexion moments. This holds true for the hips and knees. This is expected since increasing the moment arm reduces the force required to pedal. The moments at the ankles were not different across all trials. This could indicate that because of the limited mobility of the ankles, the effects of the differential stride lengths can mainly be observed in the hips and knees which compensate for the lack of mobility.

In trial II, all joints across both legs showed similar patterns. There were some differences between the peak moments but not large enough compared to trials I and III.

Similar to trial I, trial III showed that decreasing the length of the crank arm also heavily affects the internal moments at joints. The flexor moment generated at the left hip was lower throughout the gait cycle and the peak was 30% less than that of the right hip. Similar patterns were observed at the knee joint. As in trial I, the decrease of the moment

arm led to an increase in internal moments. It is worth noting that the magnitude of the moments in trial III were larger than in trial I as well.

A few studies have compared elliptical training to over-ground walking [69, 70, 71]. Yet only one of them examined the moments while the rest focus on the kinematics and EMG in lower extremities. One study compared joint moments during stepping motion and elliptical motion, but both were performed on the same elliptical trainer [72]. Overall, only three studies thus far have examined joint moments during elliptical training.

The joint moments for Motogaitor exercise calculated through inverse dynamics fall within range of the values reported in literature. The patterns observed in each gait plot match the findings of Lu and Chien. [70]. However, these patterns differed from the findings of Knutzen et al [73] with the exception of the ankle joint moment plot and differed completely from the findings of Rgoatzki et al [72]. It is also worth noting that the gait patterns were not similar across these studies. These differences, however, could be attributed to the fact that a different elliptical trainer was used in each study. Knutzen et al. performed their study using Precor EFX 546 elliptical (Precor, Woodinville, WA). This device allows for adjustable stride lengths, but in their study, they used a fixed stride length. The device also uses fixed handlebars, which eliminates upper body motion. The users operated the device at 120 strides per minute. Rogatzki et al. used Precor Adaptive Motion Trainer, which has a wider range of stride lengths. The authors state the handles were not used on the machine during the experiment. Lu and Chien used a commercially available device, but no information about the device can be found online. The users in the experiment pedal at 50 RPM.

It can also be hypothesized that individuals in each study including the present one has different strategies when exercising such as shifting the body weight to the leg in the stance phase. Lastly, the motor assistance is a confounding variable that could have affected the results of this study. Since none of the aforementioned studies had motor assistance, we expect that allowing the user to drive the motion would generate higher moments at the joints.

CHAPTER 8

CONCLUSIONS

The goal of this study was to establish an approach to collect ground reaction forces and marker trajectories to apply an inverse dynamics routine to quantify internal moments at lower extremities and compare them to ambulation. We also aimed to investigate the effects of having differential stride lengths in our elliptical, the Motogaitor, on moments at the hips, knees, and ankles. Our results indicate that elliptical exercise differs from walking by limiting the motion of the ankles, which in turn causes an increase in extensor moments at the knee and a significant decrease in plantarflexor moments. Additionally, we concluded that increasing the length of the crank arm does in fact reduce the internal moment in the affected limb.

Limitations

We tested the device on a small test sample (n=1) however future work with test on more individuals. The present study helped to define quantitative data collection procedures of this novel device. The participant did not overcome the motor and free wheel at a targeted RPM. Based on the limited time and current COVID restrictions we were unable to collect more data. We still observed some differences in net lower extremity joint moments bilaterally that may be enhanced when the participant exceeds the assistive motor. Future iterations of the device will include a display to provide the

number of RPMs utilized while operating the device allowing the participants to target peddling intensities.

Future Work

The present case study provides a preliminary insight on Motogaitor exercise compares to over-ground walking in terms of joint moments. It also examines the effects of having differential stride lengths on joint moments in each leg. While the ranges for joint moments were consistent with previous literature, the patterns in the gait plot matched the ones found in one study and differed from the rest [70]. This is research can be further expanded by accounting for some of the variables that were not accounted for in previous studies. One, data should be collected from participants with different heights to gain a better understanding of how the relative size of their segments could change the location of the hip relative to the foot during a gait cycle. This is important since the hip moment relies on the position of the hip in relation to the foot [74]. Second, the effects of the motor-assistance should be examined by collecting data with the motor-assistance and then comparing it to data collected during "freewheeling." When the user is driving the motion (i.e.: freewheeling), the crank is moving faster than the motor. Thus, we expect higher joint moments than when it is driven by the motor. Third, Chien et al. concluded that reducing the slope of the ellipse may reduce harmful joint loadings [70]. As such, the effects of changing the diameter of ellipse (i.e.: Changing the length of the crank on both sides) and comparing the joint moments across the different stride lengths is necessary to see if that applies to the Motogaitor as well.

LIST OF REFERENCES

1. Damiano, D. L., Norman, T., Stanley, C. J., & Park, H. S. (2011). Comparison of elliptical training, stationary cycling, treadmill walking and overground walking. Gait & posture, 34(2), 260-264.
2. Yen, S. C., Schmit, B. D., & Wu, M. (2015). Using swing resistance and assistance to improve gait symmetry in individuals post-stroke. Human movement science, 42, 212-224.
3. Know Your Target Heart Rates for Exercise, Losing Weight and Health. (2020). Retrieved 4 March 2020, from https://www.heart.org/en/healthy-living/fitness/fitness-basics/target-heart-rates
4. Crawford, A., Hollingsworth, H. H., Morgan, K., & Gray, D. B. (2008). People with mobility impairments: Physical activity and quality of participation. *Disability and health journal*, *1*(1), 7-13.
5. van der Ploeg, Hidde P., et al. "Physical activity for people with a disability: a conceptual model." *Sports Medicine*, vol. 34, no. 10, 2004, p. 639+. *Gale OneFile: Health and Medicine*, https://link.gale.com/apps/doc/A200844808/HRCA?u=birm97026&sid=HRCA&xid=a4f428ac. Accessed 31 Jan. 2020.
6. D. Maltais, L. Wiart, E. Fowler, O. Verschuren and D. Damiano, "Health-Related Physical Fitness for Children With Cerebral Palsy", *Journal of Child Neurology*, vol. 29, no. 8, pp. 1091-1100, 2014..
7. R. Shephard, "Physical Activity, Fitness, and Health: The Current Consensus", *Quest*, vol. 47, no. 3, pp. 288-303, 1995.

8. Martínez-González, M. Á., Martinez, J. A., Hu, F. B., Gibney, M. J., & Kearney, J. (1999). Physical inactivity, sedentary lifestyle and obesity in the European Union. *International journal of obesity*, *23*(11), 1192-1201.

9. Hu, F. B. (2003). Sedentary lifestyle and risk of obesity and type 2 diabetes. *Lipids*, *38*(2), 103-108.

10. Rosenberg, D. E., Bombardier, C. H., Artherholt, S., Jensen, M. P., & Motl, R. W. (2013). Self-reported depression and physical activity in adults with mobility impairments. *Archives of Physical Medicine and Rehabilitation*, *94*(4), 731-736.

11. Lotan, M., Isakov, E., & Merrick, J. (2004). Improving functional skills and physical fitness in children with Rett syndrome. *Journal of Intellectual Disability Research*, *48*(8), 730-735.

12. Powell, K. E., & Blair, S. N. (1994). *The public health burdens of sedentary living habits: theoretical but realistic estimates*. Medicine and science in sports and exercise, 26(7), 851-856.

13. National Multiple Sclerosis Society. MS prevalence. Available at: http://www.nationalmssociety.org/about-the-society/ms-prevalence/ index.aspx. Accessed October 10. 2020.

14. Fox R. Multiple sclerosis. Cleveland Clinic Foundation Disease Management Project. Cleveland: Cleveland Clinic; 2010.

15. Bernhard M, Gries A, Kremer P, et al. Spinal cord injury (SCI)d prehospital management. Resuscitation 2005.

16. Braddom R. Physical medicine and rehabilitation. 2nd ed. Philadelphia: WB Saunders; 2000. p 1236.

17. Delgado and A. Albright, "Movement Disorders in Children: Definitions, Classifications, and Grading Systems", Journal of Child Neurology, vol. 18, no. 1, pp. S1-S8, 2003.

18. R. Palisano, P. Rosenbaum, S. Walter, D. Russell, E. Wood and B. Galuppi, "Development and reliability of a system to classify gross motor function in children with cerebral palsy", *Developmental Medicine & Child Neurology*, vol. 39, no. 4, pp. 214-223, 2008.

19. L. Wagner and J. Davids, "Assessment Tools and Classification Systems Used For the Upper Extremity in Children With Cerebral Palsy", *Clinical Orthopaedics and Related Research®*, vol. 470, no. 5, pp. 1257-1271, 2011.

20. N. Tsorlakis, C. Evaggelinou, G. Grouios and C. Tsorbatzoudis, "Effect of intensive neurodevelopmental treatment in gross motor function of children with cerebral palsy", *Developmental Medicine & Child Neurology*, vol. 46, no. 11, 2004.

21. Butler and J. Darrah, "Effects of neurodevelopmental treatment (NDT) for cerebral palsy: an AACPDM evidence report", *Developmental Medicine and Child Neurology*, vol. 43, no. 11, p. 778, 2001. Available: 10.1017/s0012162201001414.

22. E. Fowler, T. Ho, A. Nwigwe and F. Dorey, "The Effect of Quadriceps Femoris Muscle Strengthening Exercises on Spasticity in Children With Cerebral Palsy", *Physical Therapy*, vol. 81, no. 6, pp. 1215-1223, 2001. Available: 10.1093/ptj/81.6.1215.

23. C. Andersson, W. Grooten, M. Hellsten, K. Kaping and E. Mattsson, "Adults with cerebral palsy: walking ability after progressive strength training", *Developmental Medicine & Child Neurology*, vol. 45, no. 04, 2003. Available: 10.1017/s0012162203000446.

24. Seshadri, S., Beiser, A., Kelly-Hayes, M., Kase, C. S., Au, R., Kannel, W. B., & Wolf, P. A. (2006). The lifetime risk of stroke: estimates from the Framingham Study. *Stroke, 37*(2), 345-350.

25. Ade-Hall, R. and P. Moore, *Botulinum toxin type A in the treatment of lower limb spasticity in cerebral palsy*. Cochrane Database of Systematic Reviews, 2000(1).

26. Butler, C. and S. Campbell, *Evidence of the effects of intrathecal baclofen for spastic and dystonic cerebral palsy*. Developmental Medicine & Child Neurology, 2000. 42(9): p. 634-645.

27. Damiano, D.L., *Activity, Activity, Activity: Rethinking Our Physical Therapy Approach to Cerebral Palsy*. *Physical Therapy, 2006. 86(11): p. 1534-1540.*

28. *United States Department of Health and Human Servi*ces. Physical Activity Guidelines for Americans,. 2008 [cited 2019; Available from: https://health.gov/paguidelines/2008/.

29. Sit, C.H., et al., *Physical Activity and Sedentary Time among Children with Disabilities at School*. Med Sci Sports Exerc, 2017. 49(2): p. 292-297.

30. Wist, S., Clivaz, J., & Sattelmayer, M. (2016). Muscle strengthening for hemiparesis after stroke: A meta-analysis. Annals of physical and rehabilitation medicine, 59(2), 114-124.

31. Urimubenshi, G. (2015). Activity limitations and participation restrictions experienced by people with stroke in Musanze district in Rwanda. *African health sciences*, *15*(3), 917-924.

32. Skilbeck, C. E., Wade, D. T., Hewer, R. L., & Wood, V. A. (1983). Recovery after stroke. *Journal of Neurology, Neurosurgery & Psychiatry*, *46*(1), 5-8.

33. Pinto, C. B., Saleh Velez, F. G., Lopes, F., de Toledo Piza, P. V., Dipietro, L., Wang, Q. M., ... & Fregni, F. (2017). SSRI and motor recovery in stroke: reestablishment of inhibitory neural network tonus. *Frontiers in neuroscience*, *11*, 637.

34. Claflin, E. S., Krishnan, C., & Khot, S. P. (2015). Emerging treatments for motor rehabilitation after stroke. *The Neurohospitalist*, *5*(2), 77-88.

35. Yen, S. C., Schmit, B. D., Landry, J. M., Roth, H., & Wu, M. (2012). Locomotor adaptation to resistance during treadmill training transfers to overground walking in human SCI. *Experimental brain research*, *216*(3), 473-482.

36. DeLisa, J. A. (Ed.). (1998). *Gait analysis in the science of rehabilitation* (Vol. 2). Diane Publishing.

37. Carse, B., Meadows, B., Bowers, R., & Rowe, P. (2013). Affordable clinical gait analysis: An assessment of the marker tracking accuracy of a new low-cost optical 3D motion analysis system. *Physiotherapy*, *99*(4), 347-351

38. Walker, C. R. C., Myles, C., Nutton, R., & Rowe, P. (2001). Movement of the knee in osteoarthritis: the use of electrogoniometry to assess function. *The Journal of bone and joint surgery. British volume*, *83*(2), 195-198.

39. Rowe, P. J., Myles, C. M., Hillmann, S. J., & Hazlewood, M. E. (2001). Validation of flexible electrogoniometry as a measure of joint kinematics. *Physiotherapy*, *87*(9), 479-488.

40. Gage, J. R. (1993). Gait analysis. An essential tool in the treatment of cerebral palsy. *Clinical orthopaedics and related research*, (288), 126-134.

41. Gage, J. R., Perry, J., Hicks, R. R., Koop, S., & Werntz, J. R. (1987). Rectus femoris transfer to improve knee function of children with cerebral palsy. *Developmental Medicine & Child Neurology*, *29*(2), 159-166.

42. Brunner, R., Meier, G., & Ruepp, T. (1998). Comparison of a stiff and a spring-type ankle-foot orthosis to improve gait in spastic hemiplegic children. *Journal of Pediatric Orthopaedics*, *18*(6), 719-726.

43. Bennett, B. C., Russell, S. D., & Abel, M. F. (2012). The effects of ankle foot orthoses on energy recovery and work during gait in children with cerebral palsy. *Clinical Biomechanics*, *27*(3), 287-291.

44. Neptune, R. R., Kautz, S. A., & Zajac, F. E. (2001). Contributions of the individual ankle plantar flexors to support, forward progression and swing initiation during walking. *Journal of biomechanics*, *34*(11), 1387-1398.

45. Allen, J. L., Kautz, S. A., & Neptune, R. R. (2011). Step length asymmetry is representative of compensatory mechanisms used in post-stroke hemiparetic walking. *Gait & posture*, *33*(4), 538-543.

46. Taylor, N.F., et al., *Progressive resistance training and mobility-related function in young people with cerebral palsy: a randomized controlled trial*. Dev Med Child Neurol, 2013. 55(9): p. 806-12.

47. Lauruschkus, K., et al., *Participation in physical activities for children with cerebral palsy: feasibility and effectiveness of physical activity on prescription*. Archives of physiotherapy, 2017. 7: p. 13-13.

48. Prosser, L.A., et al., *Comparison of elliptical training, stationary cycling, treadmill walking and overground walking. Electromyographic patterns*. Gait Posture, 2011. 33(2): p. 244-50

49. "ICARE: The Intelligently Controlled Assistive Rehabilitation Elliptical - T", *Madonna Rehabilitation Hospitals*, 2020. [Online]. Available: https://www.madonna.org/technology/icare-the-intelligently-controlled-assistive-rehabilitation-elliptical. [Accessed: 14- Jan- 2020].

50. Burnfield, J., et al., Walking and Fitness Improvements in a Child With Diplegic Cerebral Palsy Following Motor-Assisted Elliptical Intervention. Vol. 30. 2018. E1-E7.

51. M. Group, "Innowalk | Made for Movement", *Madeformovement.com*, 2020. [Online]. Available: https://www.madeformovement.com/innowalk. [Accessed: 14- Jan- 2020].

52. M. Yazıcı, A. Livanelioğlu, K. Gücüyener, L. Tekin, E. Sümer and Y. Yakut, "Effects of robotic rehabilitation on walking and balance in pediatric patients with hemiparetic cerebral palsy", *Gait & Posture*, vol. 70, pp. 397-402, 2019. Available: 10.1016/j.gaitpost.2019.03.017.

53. "Lokomat® - Hocoma", *Hocoma*, 2020. [Online]. Available: https://www.hocoma.com/us/solutions/lokomat/. [Accessed: 14- Jan- 2020].

54. S. Jezernik, G. Colombo, T. Keller, H. Frueh, and M. Morari, “Robotic Orthosis Lokomat: A Rehabilitation and Research Tool,” Neuromodulation: Technology at the Neural Interface, vol. 6, no. 2, pp. 108–115, 2003.

55. “Products, Education and Rehabilitation Solutions,” *LiteGait.com | Products, Education and Rehabilitation Solutions*. [Online]. Available: https://www.litegait.com/. [Accessed: 14-Jan-2020].

56. J. Hidler, D. Brennan, I. Black, D. Nichols, K. Brady, and T. Nef, “ZeroG: Overground gait and balance training system,” *The Journal of Rehabilitation Research and Development*, vol. 48, no. 4, p. 287, 2011.

57. “Pacer Gait Trainers,” *Rifton*. [Online]. Available: https://www.rifton.com/products/gait-trainers/pacer-gait-trainers. [Accessed: 14-Jan-2020].

58. Karatsidis, A., Bellusci, G., Schepers, H. M., De Zee, M., Andersen, M. S., & Veltink, P. H. (2017). Estimation of ground reaction forces and moments during gait using only inertial motion capture. *Sensors*, *17*(1), 75.

59. Van Ingen Schenau, G. V., Bobbert, M. F., & Rozendal, R. H. (1987). The unique action of bi-articular muscles in complex movements. *Journal of anatomy*, *155*, 1.

60. Tuan, L. V., Ohnishi, K., Otsuka, H., Agarie, Y., Yamamoto, S., & Hanafusa, A. (2017). Finite element analysis for the estimation of the ground reaction force and pressure beneath the foot prosthesis during the gait of transfemoral patients. In *Journal of Biomimetics, Biomaterials and Biomedical Engineering* (Vol. 33, pp. 1-11). Trans Tech Publications Ltd.

61. Eng, J. J., & Winter, D. A. (1995). Kinetic analysis of the lower limbs during walking: what information can be gained from a three-dimensional model?. *Journal of biomechanics*, *28*(6), 753-758.

62. Reilly, D. T., & Martens, M. (1972). Experimental analysis of the quadriceps muscle force and patello-femoral joint reaction force for various activities. Acta Orthopaedica Scandinavica, 43(2), 126-137.

63. Lay, A. N., Hass, C. J., & Gregor, R. J. (2006). The effects of sloped surfaces on locomotion: a kinematic and kinetic analysis. Journal of biomechanics, 39(9), 162.

64. Sutherland, D. H., Olshen, R. I. C. H. A. R. D., Cooper, L., & Woo, S. L. (1980). The development of mature gait. J Bone Joint Surg Am, 62(3), 336-353.

65. Pierson-Carey, C. D., Brown, D. A., & Dairaghi, C. A. (1997). Changes in resultant pedal reaction forces due to ankle immobilization during pedaling. Journal of Applied Biomechanics, 13(3), 334-346.
66. Simonsen, E. B., Svendsen, M. B., Nørreslet, A., Baldvinsson, H. K., Heilskov-Hansen, T., Larsen, P. K., ... & Henriksen, M. (2012). Walking on high heels changes muscle activity and the dynamics of human walking significantly. *Journal of applied biomechanics*, *28*(1), 20-28.
67. Mughal MZ. Fractures in children with cerebral palsy. Curr Osteoporos Rep. 2014 Sep;12(3):313-8. doi: 10.1007/s11914-014-0224-1.
68. Farris, DJ, Hampton, A, Lewek, MD, and Sawicki, GS. Revisiting the mechanics and energetics of walking in individuals with chronic hemiparesis following stroke: from individual limbs to lower limb joints. J Neuroeng Rehabil. 2015; 12: 24.
69. Prosser, L. A., Stanley, C. J., Norman, T. L., Park, H. S., & Damiano, D. L. (2011). Comparison of elliptical training, stationary cycling, treadmill walking and overground walking. Electromyographic patterns. *Gait & posture*, *33*(2), 244-250.
70. Lu, T., Chien, H., & Chen, H. (2007). Joint loading in the lower extremities during elliptical exercise. *Medicine and science in sports and exercise*, *39*(9), 1651.
71. Burnfield, J. M., Cesar, G. M., Buster, T. W., Irons, S. L., & Nelson, C. A. (2017). Kinematic and muscle demand similarities between motor-assisted elliptical training and walking: Implications for pediatric gait rehabilitation. *Gait & posture*, *51*, 194-200.
72. Rogatzki, M. J., Kernozek, T. W., Willson, J. D., Greany, J. F., Hong, D. A., & Porcari, J. P. (2012). Peak muscle activation, joint kinematics, and kinetics during elliptical and stepping movement pattern on a Precor Adaptive Motion Trainer. *Research quarterly for exercise and sport*, *83*(2), 152-159.
73. M Knutzen, K., L McLaughlin, W., J Lawson, A., S Row, B., & Tyson Martin, L. (2010). Influence of ramp position on joint biomechanics during elliptical trainer exercise. *The Open Sports Sciences Journal*, *3*(1).

74. Ounpuu, S., Davis, R. B., & Deluca, P. A. (1996). Joint kinetics: methods, interpretation and treatment decision-making in children with cerebral palsy and myelomeningocele. *Gait & posture*, *4*(1), 62-78.

APPENDIX A

FIGURES

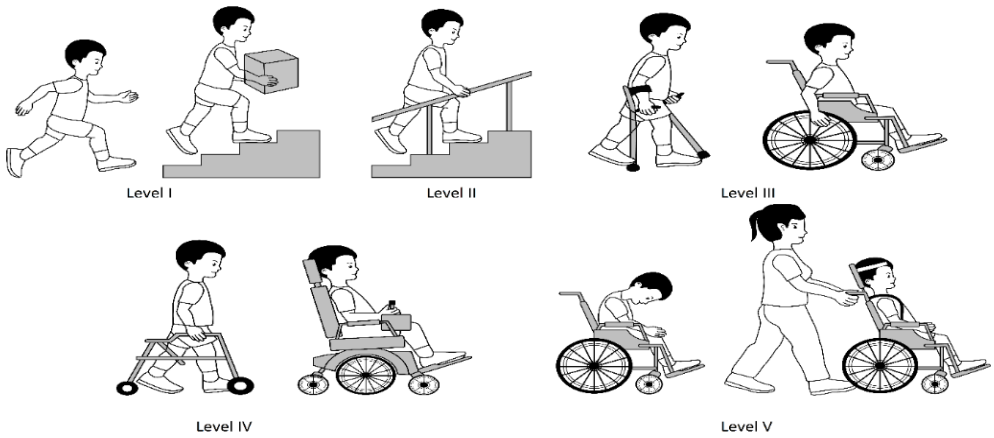

Figure 4. Demonstrates the five levels of CP according to the GMFCS.

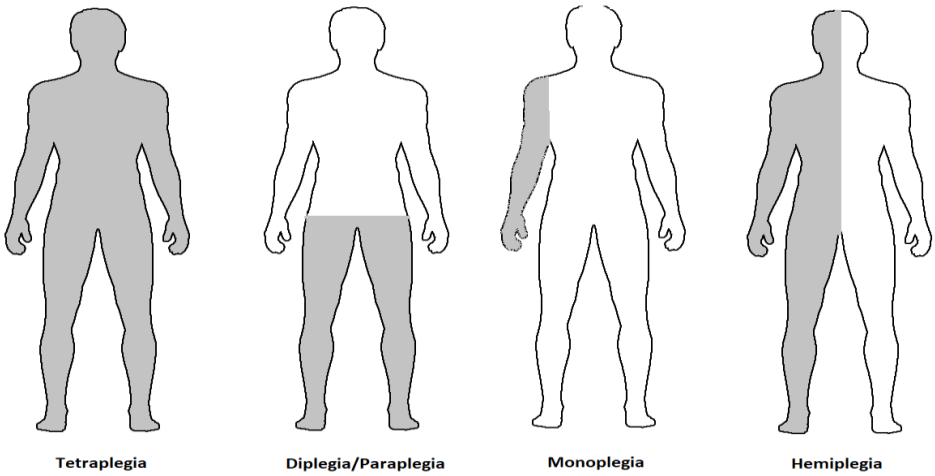

Figure 5. Classification of mobility impairments based on the affected limb(s).

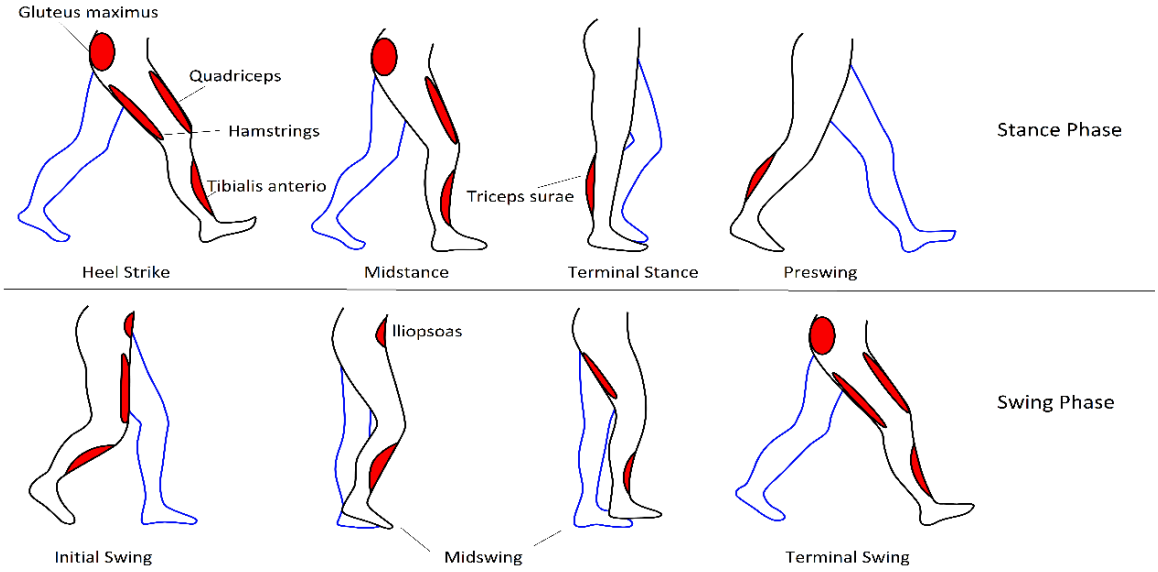

Figure 6. Demonstrates the stages of the gait cycle and the main muscles activated in each stage.

Figure 4. The E872 ICARE elliptical machine, the Innowalk, and the Lokomat [49, 51, 53].

Figure 5. Displays the pediatric LiteGait and the Rifton Pacer [55, 57].

Figure 6. The CAD model of the Motogaitor (left) and the client using the device (right).

Figure 7. The new design concept with the bicycle freewheel sprocket.

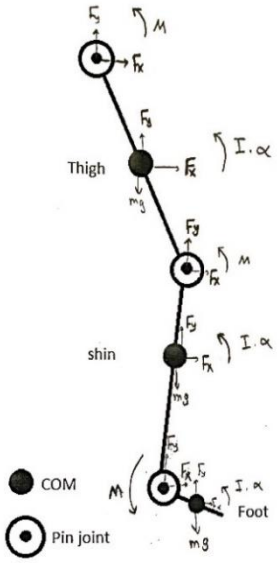

Figure 8. 2-D segmented model of a leg showing the forces and moments at every joint and COM

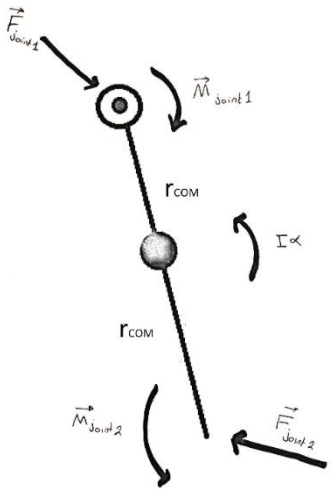

Figure 9. A free-body diagram of the calf segment

Figure 10. Hough Transform creating black/white image for edge extraction and angle estimation.

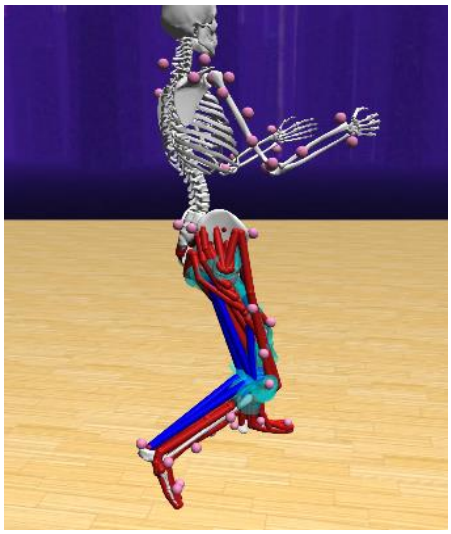

Figure 11. OpenSim model with the spastic muscles associated with the stiff knee (highlighted in blue).

Figure 12. The load cells sandwiched between two plates.

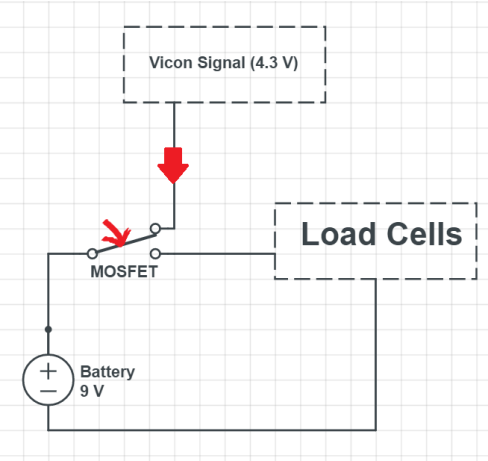

Figure 13. MOSFET circuit where the signal is generated from the Vicon triggering the MOSFET, thus allowing the battery to initiate data collection from the load cells.

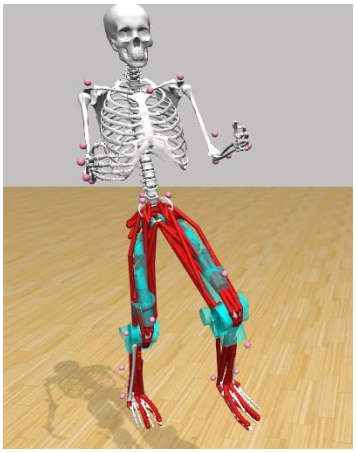

Figure 14. OpenSim model with the markers.

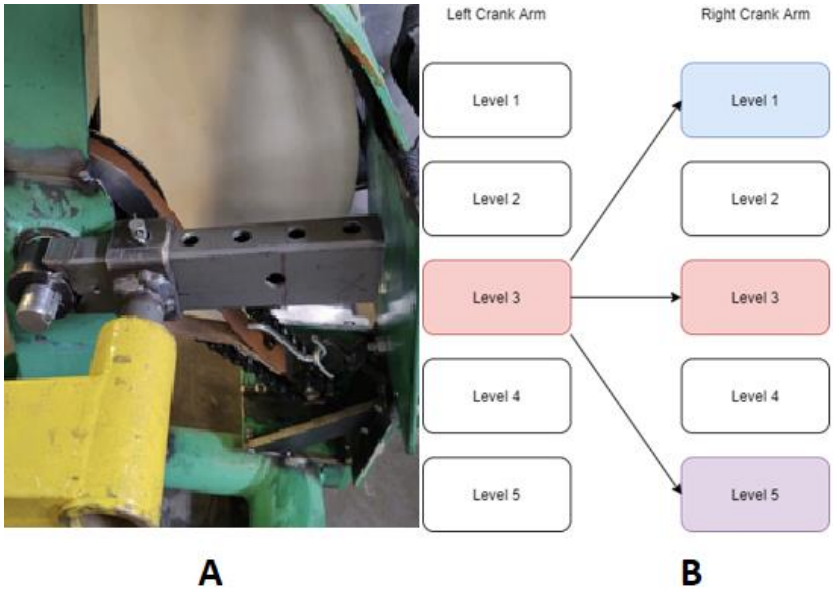

Figure 15. (A) Shows the crank arm. (B) How the trials for the differential stride lengths were performed.

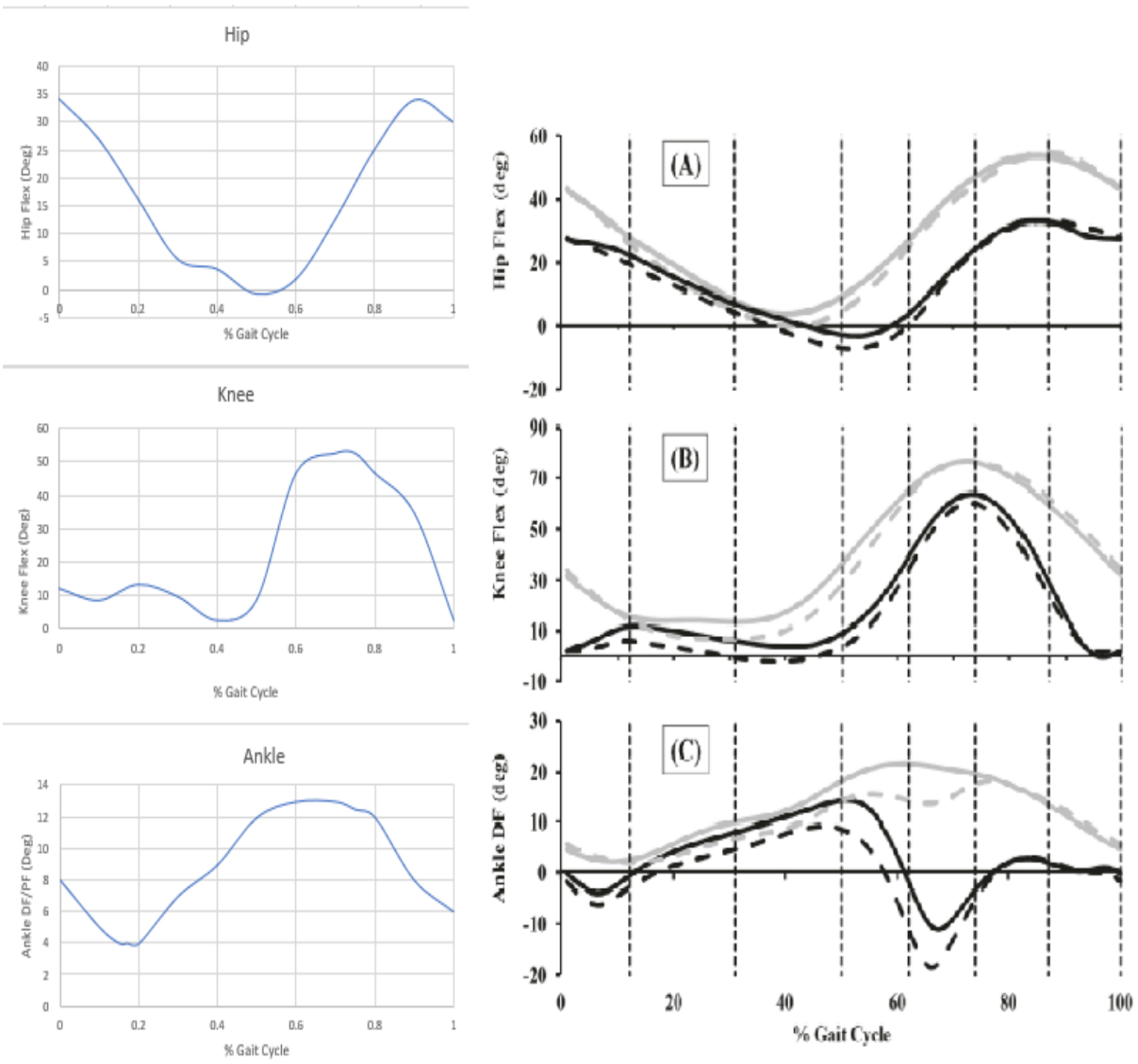

Figure 76. Joint kinematics of the TD model using the Motogaitor in the sagittal plane compared to Buster et al [71].

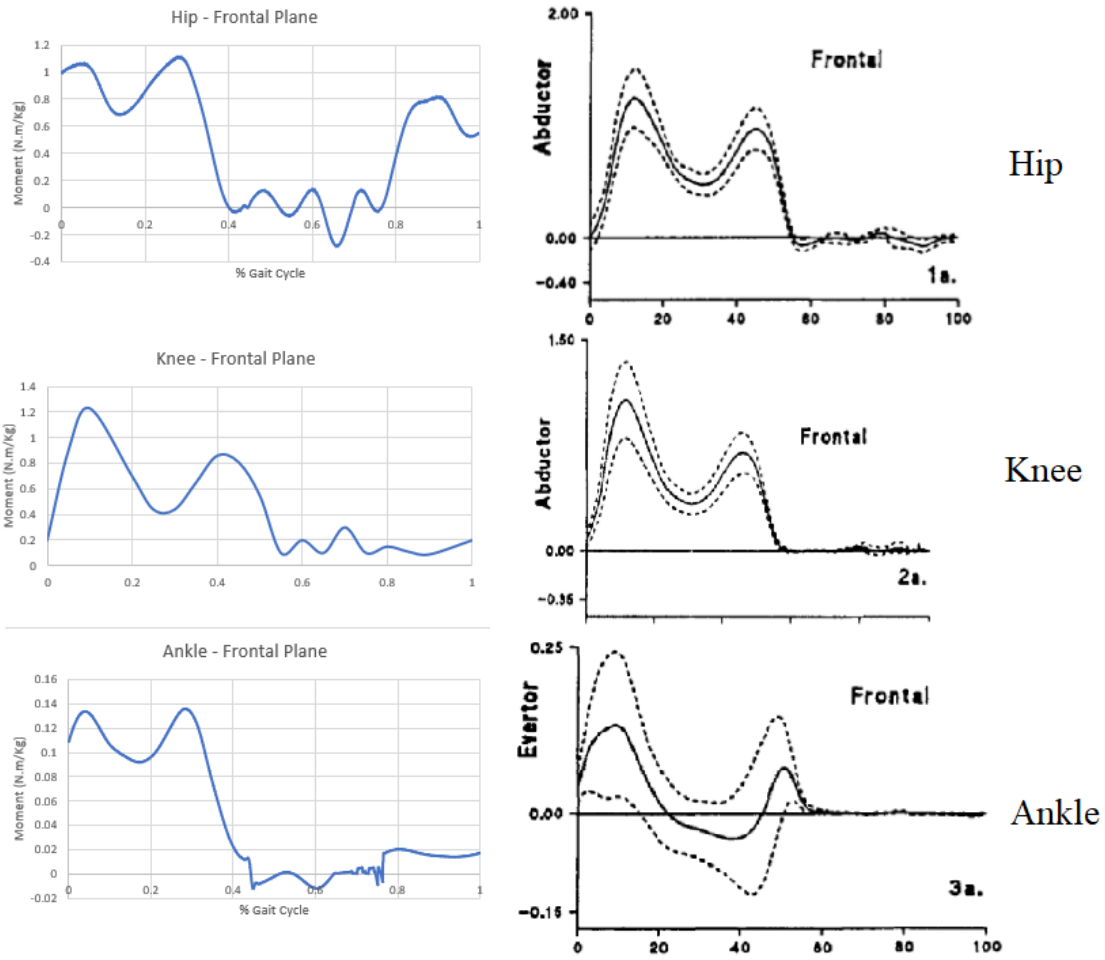

Figure 17. Joint kinetics of the TD model using the Motogaitor in the frontal plane compared to the results of Winter [69].

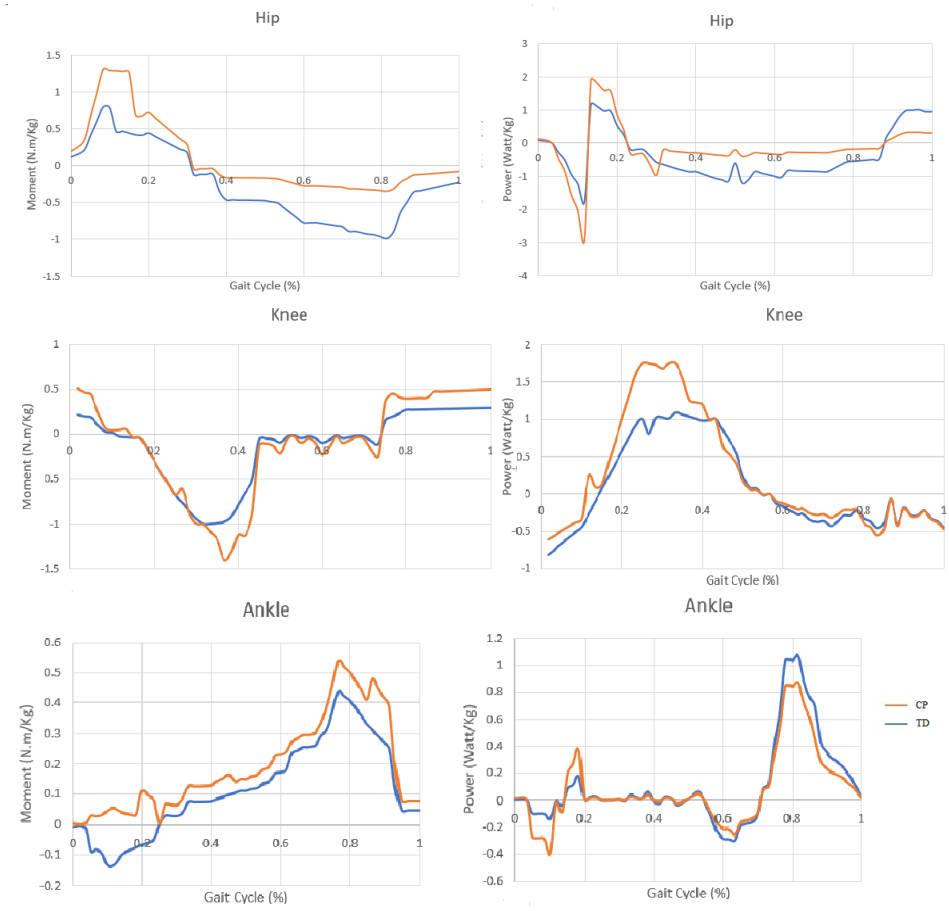

Figure 18. Moment and power gait plots for the CP and TD models in the Motogaitor simulation.

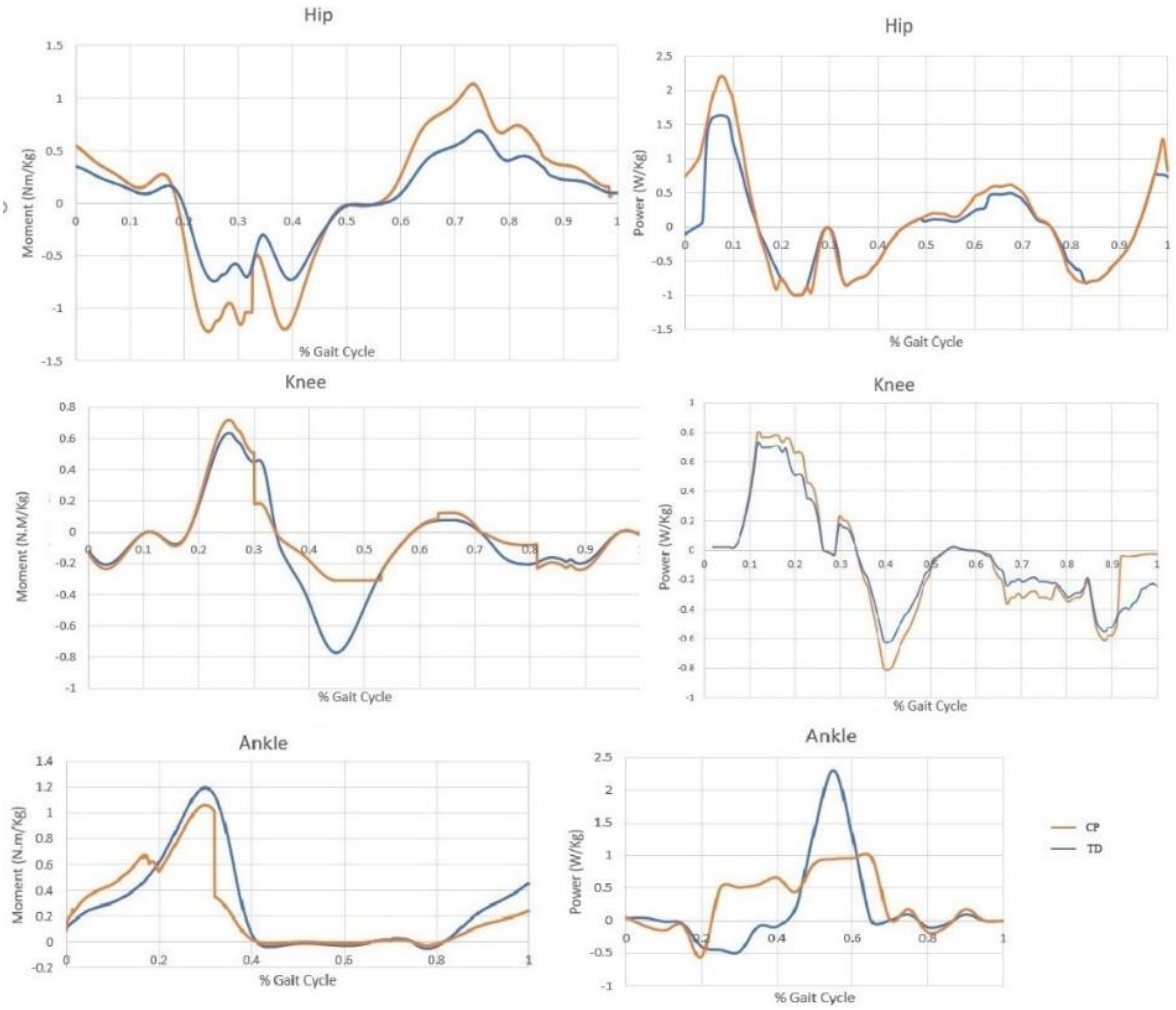

Figure 19. Moment and power gait plots for the CP and TD models during normal walking.

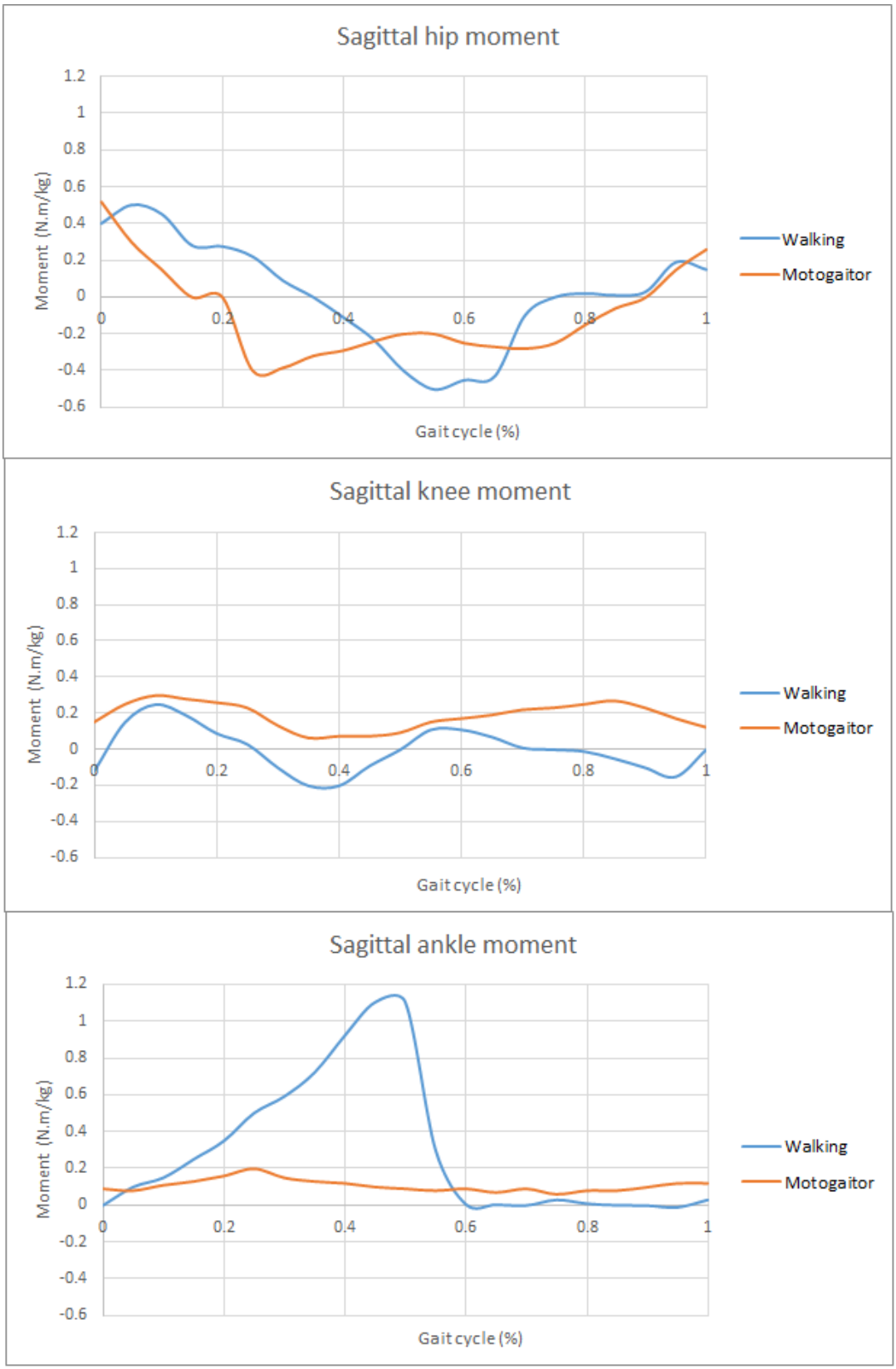

Figure 20. Compares sagittal plane joint moments in walking and Motogaitor exercise.

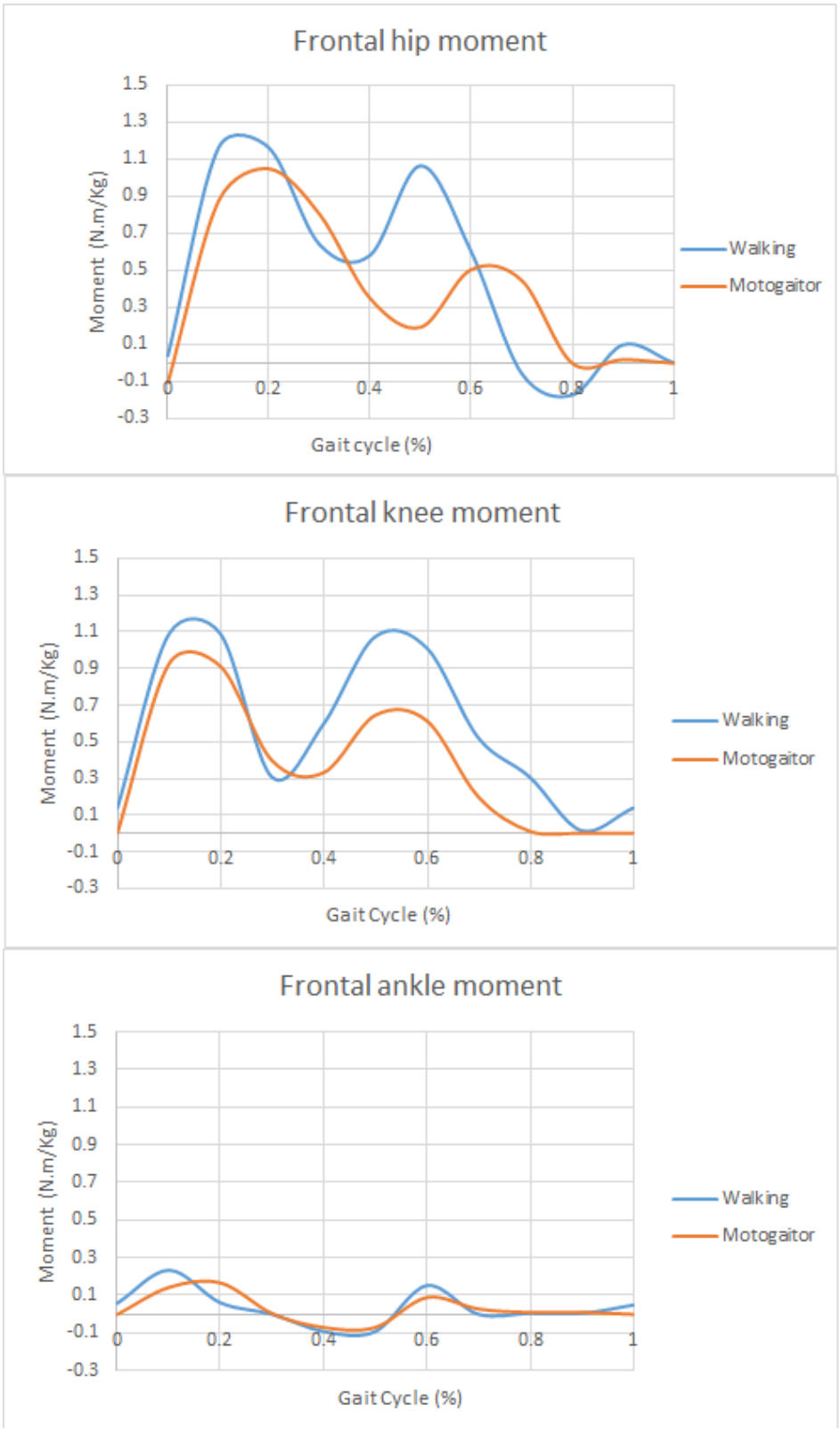

Figure 21. Compares frontal plane joint moments in walking and Motogaitor exercise.

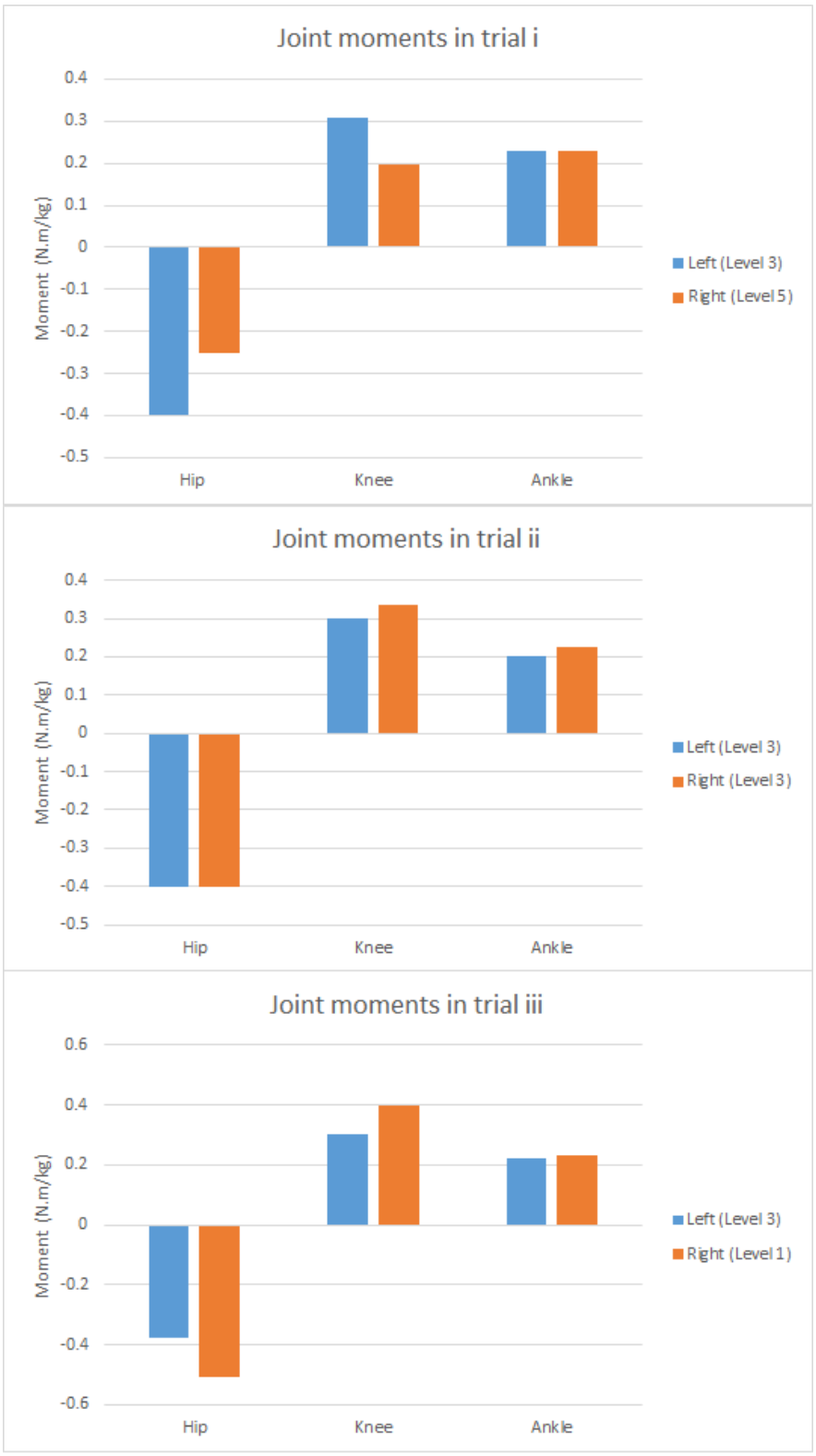

Figure 22. Displays the change in peak joint moments in both legs with the change in crank arm length.

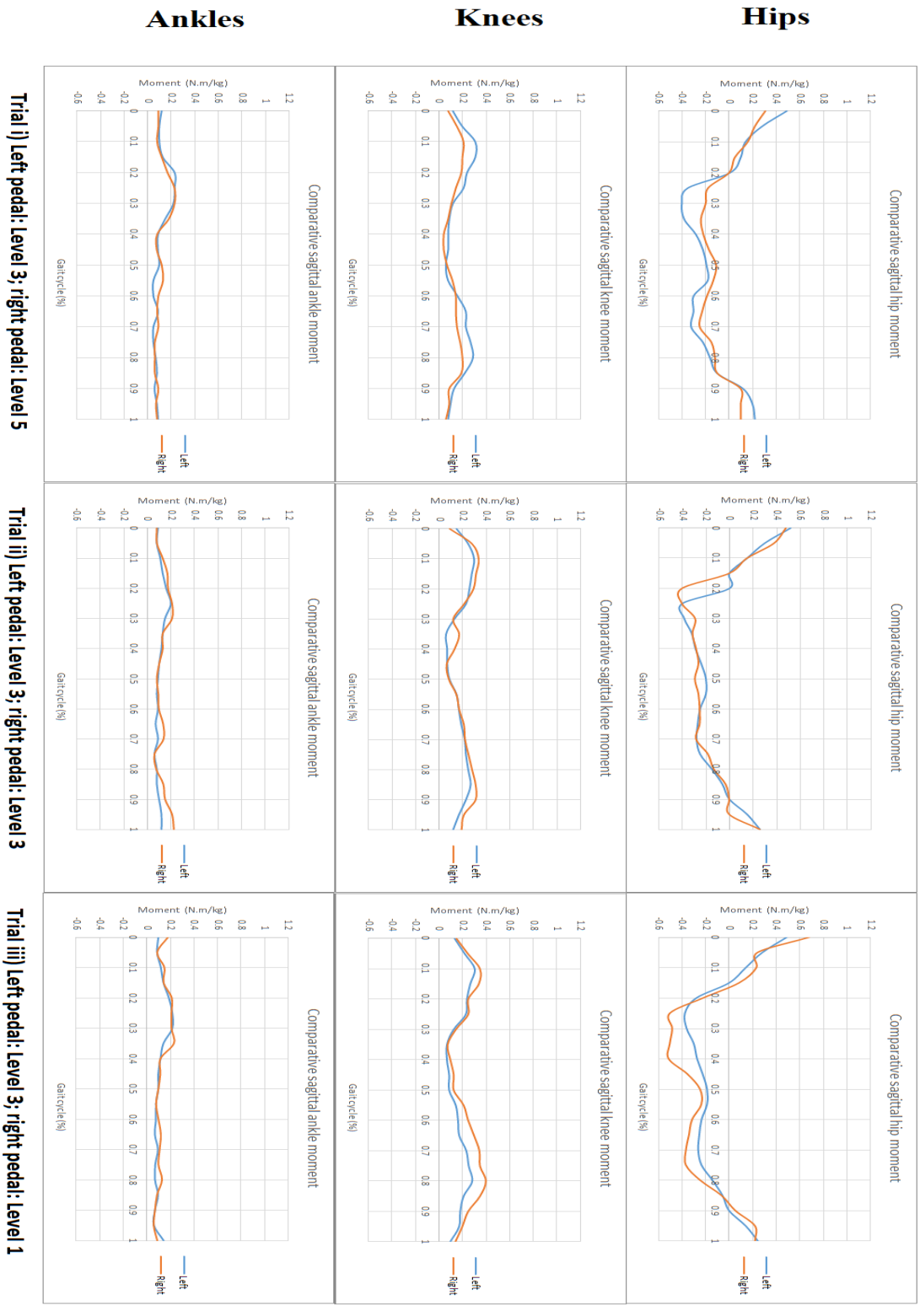

Figure 23. Joint moments due to the change in crank arm length in Motogaitor exercise.

APPENDIX B

TABLES

Table 1. Feedback from the user-testing that led to the new design constraints.

`	1	2	3	4	5	6
Weight (lbs.)	58	20	23	24	32	36
Height (In.)	48	29	32	N/A	36	38
Age (mo.)	144	16	19	16	24	72
Diagnosis	Level V CP and hydrocephalus	CP - Level unknown	Dandy Walker Syndrome and Developmental Delays	Congenital Hydrocephalus	Left hemiparesis and seizures	Triplegic Spastic CP
Feedback	User Velcro grips similar to Rifton	Better if one person could place child in device	Felt that child was very comfortable in the device	Speed settings are ideal	Could be a little smaller around the waist	Better if it could be interchangeable with variety of walkers and had easier entry
Price	$3,000 to $5,000	N/A	$2000	$2000 - $3000	$200	$1000

Table 2. Peak moments in the hip joint in over-ground walking and Motogaitor exercise for TD and CP.

	Motogaitor				Over-ground walking			
	TD		CP		TD		CP	
Moment type	Extensor (+)	Flexor (-)	Extensor (+)	Flexor (-)	Extensor (+)	Flexor (-)	Extensor (+)	Flexor (-)
Moments (N.m/Kg)	0.788	-0.949	1.35	-0.32	0.539	-0.549	1.37	-0.549

Table 3. Peak moments in the knee joint in over-ground walking and Motogaitor exercise for TD and CP.

	Motogaitor				Over-ground walking			
	TD		CP		TD		CP	
Moment type	Extensor (+)	Flexor (-)	Extensor (+)	Flexor (-)	Extensor (+)	Flexor (-)	Extensor (+)	Flexor (-)
Moments (N.m/Kg)	0.383	-1.01	0.488	-1.45	0.67	-0.78	0.722	-0.31

Table 4. Peak moments in the ankle joint in over-ground walking and Motogaitor exercise for TD and CP.

	Motogaitor				Over-ground walking			
	TD		CP		TD		CP	
Moment type	Extensor (+)	Flexor (-)	Extensor (+)	Flexor (-)	Extensor (+)	Flexor (-)	Extensor (+)	Flexor (-)
Moments (N.m/Kg)	0.437	-0.138	0.521	N/A	1.17	0.02	1.14	0.009

Table 5. Sagittal plane joint moments during walking and Motogaitor exercise.

Exercise Type	**Hip Moment (Peak)**	**Knee Moment (Peak)**	**Ankle Moment (Peak)**
Walking	-0.520 N.m/kg	0.250 N.m/kg	1.10 N.m/kg
Motogaitor	-0.401 N.m/kg	0.299 N.m/kg	0.211 N.m/kg

Table 6. Frontal plane joint moments during walking and Motogaitor exercise.

Exercise Type	**Hip Abduction Moment (peak)**	**Knee Abduction Moment (Peak)**	**Ankle Inversion Moment (peak)**
Walking	1.16 N.m/kg	1.08 N.m/kg	0.23 N.m/kg
Motogaitor	1.04 N.m/kg	0.926 N.m/kg	0.168 N.m/kg